Statistical Modeling of Randomly Branched Polymers Produced by Combination of Several Single-Site Catalysts: Toward Optimization of Melt Properties

Stephane Costeux†

Department of Chemical Engineering, McGill University, Montreal, Quebec

Received June 3, 2002; Revised Manuscript Received December 30, 2002

ABSTRACT: A statistical model describing the polymerization of branched ethylene homopolymers from a single site catalyst (*Macromolecules* **2002**, *35*, 2514) for continuous stirred-tank reactor (CSTR) is extended to the case of a mixture of single-site catalysts in order to establish qualitative criteria to optimize the processability of branched metallocene ethylene homopolymers. Monte Carlo simulations are used for combinations of two metallocene catalysts, and an analytical solution is proposed to predict the ternary diagram of segmental composition (linear chains/free arms/inner backbones) and the molecular weight distribution for any combination of single-site catalysts. It is shown that the optimization of shear and extensional properties requires good control of the extent of vinyl termination and of the size of the segments between branch points.

Introduction

The prediction of processing properties of branched polymeric materials requires a detailed understanding of structure−property relationships. Several dynamic models have been proposed that allow the calculation of rheological properties with good accuracy for linear systems[2,3] and for simplified branched materials, usually monodisperse.[4,5] Techniques are also available to allow for polydispersity in branched systems, although the equations have to be simplified.[6]

A prerequisite for the use of these models for more complex branched systems is the knowledge of the structure of the polymer, namely the topological characteristics of the molecules. In a previous paper,[1] it was shown that the structure of a branched metallocene polyethylene (BmPE) obtained using a constrained geometry catalyst (CGC) can be described in terms that provide a qualitative estimate of behavior of the melt in shear and extensional flows.

It was shown that for a single-site catalyst based polyethylene (PE), the structure is fully described by two parameters, the average number of branch points (BP) per molecule and the average molecular weight (MW) of segments, both of which can be obtained from experimental values of long chain branching density [LCB/10^3C] and weight-average molecular weight, M_w.

We can then express the fraction (number or weight) of linear chains, free arms (attached to a branch point at one end) and inner backbones (between two branch points) in terms of the average number of BP per molecule (see Figure 1). Assuming that we can infer rheological behavior from those fractions is an approximation, since we do not consider the various types of inner backbones having different seniorities,[7] but for the levels of long chain branching achievable today, this approximation is reasonable.

Qualitatively, we can consider that free arms contribute significantly to viscosity, due to their slow relaxation process, dynamic dilution. The inner backbones have been shown to contribute significantly to strain hardening by their stretching and orientation, as pictured in the pompom model.[8] Free arms influence strain hardening only by acting as entangled anchors promoting the stretching and orientation of inner backbones, which is confirmed by the fact that melts of pure stars exhibit no strain-hardening.[9,10]

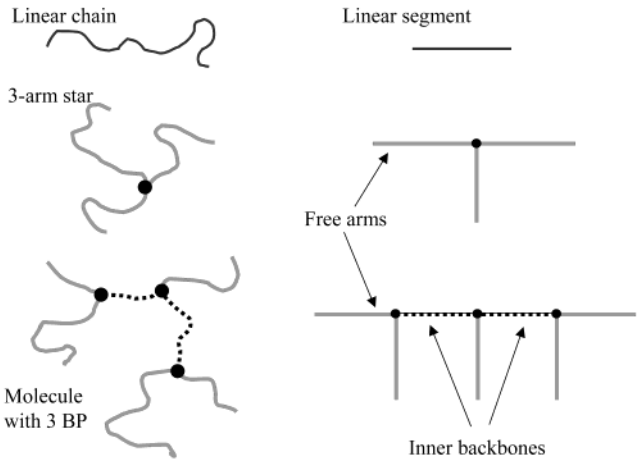

Figure 1. Description of molecular topology in terms of segments (right): linear chains are linear segments connected to 0 branch points, whereas free arms and inner backbones are segments respectively connected to 1 and 2 branch points.

Thus, increasing the fraction of inner backbones and decreasing the fraction of free arms is the key to promoting high melt strength with a reasonable melt flow rate. Despite the enormous improvement CGC catalysts have brought to the design of resins with better performance such as Dow INSITE technology[11,12] the processing properties of these materials cannot always be optimized at the same time as their performance in the solid state, because a single topological parameter controls the fractions of both inner backbones and free arms. More degrees of freedom are therefore needed to increase the ratio of inner backbones to free arms. Blending two metallocene PE is effective,[1] but this requires a separate reactor for each component, plus the mixing of two resins having different viscosities. In addition to the economical and practical drawbacks,

† Present address: The Dow Chemical Co., B-1470 Bldg, 2301 Brazosport Blvd, Freeport, TX 77541.

10.1021/ma0208640 CCC: $25.00
Published on Web 05/08/2003

there is concern about the homogeneity of such blends. Nevertheless, in some cases this may be an acceptable approach.

The combination of two or more metallocene catalysts in a single reactor is an interesting alternative. Zhu and Li[13] proposed a model for the molecular weight distribution of comb polymers obtained by a combination of two metallocene catalysts, one (linear-CGC) producing linear, vinyl-ended macromonomers and a second (LCB−CGC) having an open structure allowing the incorporation of these macromonomers. A condition for obtaining only comblike structures is that the LCB−CGC produce saturated molecules, so that only linear chains from the linear-CGC can be inserted as macromonomers. This is not easily achievable in a single-reactor, since it is difficult to control independently the rate of vinyl termination of both catalysts to obtain at the same time complete unsaturation for the linear catalyst and nearly total saturation of the branched molecules formed by the LCB−CGC. The model is nonetheless of practical interest for dual reactor synthesis.

A more realistic approach was proposed by Beigzadeh et al.[14,15] using reaction kinetics modeling for the combination of a linear-CGC and a LCB−CGC. They evaluated the effects of vinyl termination ratio between LCB−CGC and linear-CGC and mole fraction of LCB−CGC on the long-chain branching density, the polydispersity, and MW. They concluded that if the linear chains produced by the linear-CGC have a probability of vinyl termination about 5 times as large as that of molecules from the LCB−CGC, then the branching density [LCB/1000C] is increased by a factor of 4 for a molar fraction of LCB−CGC equal to 0.5, which has been nicely verified in the only experimental work on dual CGC catalyst synthesis in a single CSTR published so far.[16] However, the branching density is not strictly a topological parameter, and this optimization is dependent on the relative sizes of the linear chains from the linear-CGC and the segments between branch points produced by the LCB−CGC.

The idea of optimizing the amount of comblike molecules was recently revisited theoretically by Soares,[17] and by Monte Carlo simulations by Simon and Soares.[18] They split the branched molecules into two categories: combs, obtained when only linear branches were incorporated in the molecules, and hyperbranched molecules, obtained when at least one of the macromonomers incorporated was not linear. This provides interesting insight into the mechanisms leading to various branching structures, but it is difficult to use the results to relate these results to the melt rheological properties, because molecules with identical topologies, but created by different synthetic routes, are accounted for as either combs or hyperbranched polymers. In agreement with Zhu and Li,[13] Simon and Soares consider for instance that only a fraction of the molecules with three branch points are combs,[19] the others being hyperbranched, although one can easily check that all acyclic molecules with three branch points have the topology of a comb and therefore contribute identically to the properties of the resin.

The objective of the present work is to develop a simple probabilistic model for BmPE produced by a combination of single-site catalysts in a single reactor (CSTR) that provides a detailed topological description and that can be used to predict at least qualitatively the influence of synthesis conditions on the melt behavior in shear and extensional flow. A Monte Carlo-based combinatorial approach is used, which is somewhat similar to the "in−out" recursive method recently used by Shiau[20] for modeling random combs.

The results will be presented in terms of topological (branching probability) and dimensional (segments average molecular weight) parameters, which can be expressed as functions of the Monte Carlo propagation and monomer selection probabilities[1] for each catalyst, which are themselves related to kinetic constants.[18] The input parameters of the model can be measured experimentally using ^{13}C NMR (for branching density and vinyl termination) and by light scattering (weight-average molecular weight).

An inherent limitation of the Monte Carlo technique is that it is not adapted to batch reactor simulations, because the polymerization time does not appear as an explicit variable. Yet the probabilities of propagation and branching are functions of the polymerization time and kinetic constants, and if these functions are known (using the population balance[17] method) simulations could be carried out at various polymerization times in a batch reactor. Nevertheless the method of balance of moments mentioned above[13,16,17] is more practical for this particular case, although it cannot provide any information on segmental composition but only the evolution of average quantities with polymerization time. On the other hand, Monte Carlo simulations provide much more details on the topology of molecules, but only at a given polymerization time.

To show the effect of vinyl termination, the model will first be restricted to fully vinyl-terminated (unsaturated) molecules before implementing partial vinyl termination for a better description of the actual reactions. We will conclude by an example showing how a material could be designed to have a high melt strength with good flow properties.

The method used also offers the advantage that it need not be restricted to a combination of two catalysts, one LCB−CGC and one linear-CGC. The general case of any number, q, of LCB−CGC-type catalysts is treated, any of which can become a linear-CGC if its branching probability is set to zero. The advantage of using more than two catalysts has not yet been established, but with the increasing complexity of the reactions needed to optimize polymers, the fast growing number of catalysts available, and the imagination of organic chemists, it may become interesting in the future.

Finally, we will often refer to a site on a "single-site constrained geometry catalyst" simply as a "site", which does not imply that the model is suitable for multiple site or Ziegler−Natta catalysts, for which branching mechanisms are quite different.

Monte Carlo-Based Evaluation of Branch Structure

The procedure used to simulate a system with q sites is similar to the single-site catalyst simulation presented in ref 1, except that we now need q sets of probabilities (pp_i, lp_i), where pp_i is the propagation probability governing the total kinetic length before termination, and lp_i is the probability of propagation with an ethylene monomer rather than a macromonomer. We also need the selection probabilities ps_i that a molecule will be polymerized by site i. These probabilities are number fractions, and the sum of the ps_i is naturally equal to 1. To demonstrate the impact of each parameter, we will

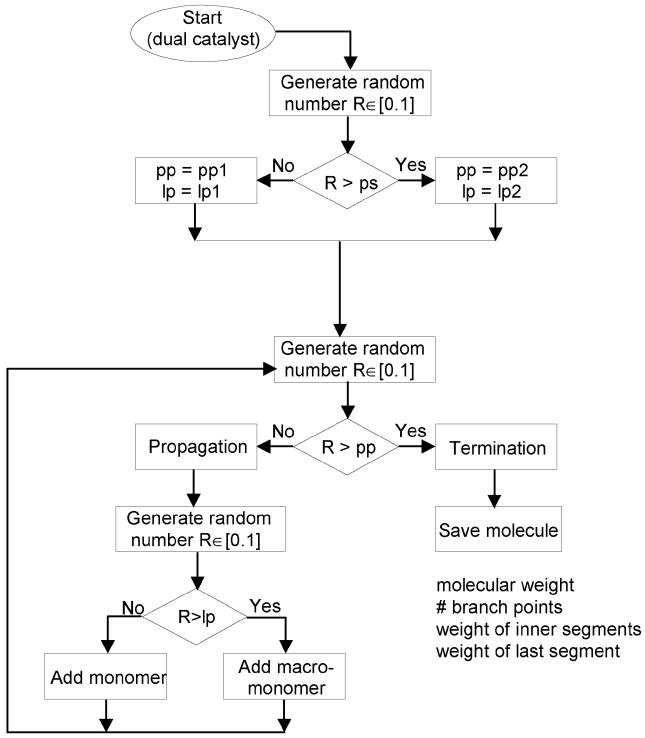

Figure 2. Algorithm of Monte Carlo simulation of a two-catalyst system.

limit the simulation to two sites, i.e., $q = 2$. All simulations were carried out with 10^6 molecules.

The parameters for the simulation are pp_1, lp_1 for site 1, pp_2, lp_2 for site 2, and the probability ps to select site 1. The process is described in Figure 2. We start by selecting a site which means picking a random number R between 0 and 1. If $R <$ ps, the molecule will be made by site 1, with pp and lp equal to pp_1 and lp_1, and if $R >$ ps by site 2. Then another random number is compared to the propagation probability pp of the selected site; if $R >$ pp, we terminate the molecule and store it. If $R <$ pp, we propagate by adding either a monomer or a macromonomer selected from the terminated molecules already stored. Finally we pick a third random number and compare it with the monomer selection probability; if $R <$ lp, we add a monomer, and if not, we incorporate a branch. When grafting a branch, we select a molecule from the set of molecules already terminated, usually the last one made, since it is as random as any other. In the single catalyst case, we stored the weight and the number of branch points of all saved molecules, so if we incorporate this molecule as a branch we can keep track of the total weight and total number of branch points of the current molecule. Knowing the number n of branch points, we have the number of inner backbones $(n - 1)$ and of free arms $(n + 2)$, which is enough to determine the segment weight fractions, since all segments have the same molecular weight distribution.

In the two-site system, sites 1 and 2 lead to different segment sizes, since for site i, we can define the number-average segment weight by

$$M_{N,Si} = \frac{28}{1 - pp_i lp_i} \tag{1}$$

where the factor 28 is the weight of an ethylene monomer. It is then more relevant to compute the weight fractions of linear molecules, free arms, and inner backbones rather than number fractions.

Therefore, we need to store the weight of the inner backbones for each branched molecule saved and the weight of the linear chains. The weight of free arms can be obtained by subtracting these two values from the total weight. The weight of linear chains being trivial to compute, we focus on the weight of inner backbones. Figure 3 shows the process of grafting a molecule already branched onto a living molecule. In the example shown, the living molecule starts its growth from the left, incorporates a first linear macromonomer, and then propagates until a second macromonomer is grafted. The segment between the two branch points, of mass m_I, will necessarily be an inner backbone, since it is trapped between two branch points. All the inner backbones of the macromonomer to be grafted will account for an additional mass $m_I^{(B)}$, because they will remain inner backbones of the growing molecule. Finally, if the macromonomer is not linear, its last segment of mass $m_V^{(B)}$, the only one being vinyl terminated, will also become an inner backbone when grafted. As a consequence, we also need to store the weight of the vinyl-terminated segment of each branched molecule. These three terms are added to get the weight of inner backbones of the living molecule, and we proceed this way until termination.

Together with this information, we keep track of the numbers of molecules and branch points, the molecular weight distributions, and other pertinent information.

In the case of incomplete vinyl termination, the program is simply modified so that at the termination of the molecule, we decide if the molecule is vinyl terminated or not by introducing a vinyl-termination probability for each catalyst, v_1 and v_2, and make the usual comparison with a random number. In a continuous, stirred-tank reactor (CSTR), these probabilities will be constant after the reaction reaches a steady state. If the molecule happens to be saturated, we store all its parameters and add its contribution to the various total weights needed for computing the averages and distributions. If the molecule is vinyl terminated, we store it in the bank of potential macromonomers.

Since they must sum to one, the weight fractions Φ_L, Φ_A, and Φ_B of linear chains, free arms, and inner backbones can be represented on a ternary diagram as shown in ref 1. To conveniently place sites 1 and 2 on the diagram, we make use of the topological parameter β_i, which would be the average number of branch points per molecule if only the site i were used:

$$\beta_i = \frac{pp_i(1 - lp_i)}{1 - 2pp_i + pp_i lp_i} \tag{2}$$

We will also use the Flory branching probability Pb_i, which relates to β_i by eq 3

$$Pb_i = \frac{pp_i(1 - lp_i)}{1 - pp_i lp_i} = \frac{\beta_i}{2\beta_i + 1} \tag{3}$$

The coordinates of site i on the ternary diagram are given by the fractions of linear molecules, free arms,

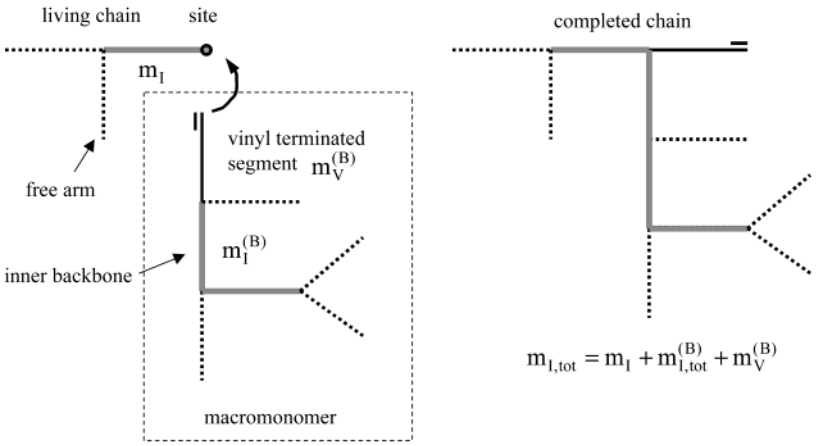

Figure 3. Method for determining weight of inner backbone by Monte Carlo simulation. Details are given in the text.

and inner backbones that it would create if it were alone in the system

$$\phi_{L,i} = \frac{\beta_i + 1}{(2\beta_i + 1)^2} \tag{4}$$

$$\phi_{A,i} = \frac{\beta_i(2\beta_i + 3)}{(2\beta_i + 1)^2} \tag{5}$$

$$\phi_{B,i} = \frac{2\beta_i^2}{(2\beta_i + 1)^2} \tag{6}$$

It is possible to accelerate the Monte Carlo algorithm significantly by using the technique suggested in ref 1. As site i produces segments following a Flory distribution, characterized by the average molecular weight $M_{N,Si}$, instead of adding monomer after monomer we can directly add segments randomly chosen according to the distribution, and decide to add a branch or terminate by comparing a random number to the branching probability Pb_i. The branch should then be chosen from the vinyl-terminated molecules already formed. Nevertheless, only the original Monte Carlo method was used to obtain the following results.

It is important to note that the values of pp_i and lp_i, or equivalently of $M_{N,Si}$ and β_i, to be input in the Monte Carlo simulation are the probabilities of catalyst i when it is mixed with the other catalysts. In the case of total vinyl termination, these values will be independent of the composition and can be determined experimentally by characterizing a resin made by catalyst i only. In the case of partial vinyl termination, we will provide a mixing rule to compute these parameters for the catalyst in a mixture with others from the values $M^*_{N,Si}$ and β_i^* when it is used alone.

Simple Case: Total Vinyl Termination

This case, although unrealistic in most situations, is useful to describe the method used subsequently. We present here a new method to elucidate the structure of branched mPE.

Let us start by assuming a different process for branching that will lead to the same final structure as that obtained using the complete Monte Carlo process. In a first step, we consider that all sites i build "main backbones" containing branch points according to their branching probability Pb_i, but that no branches are attached. When all these N main backbones are built, the second step consists of choosing for each branch point a macromonomer to be grafted as a branch. All main backbones are candidates to become branches, since all of them are vinyl terminated. The grafting process continues until all branch points in the system have a branch grafted.

We start by defining the probability $b_i(m)$ that site i produces a main backbone with m branch points, i.e., $m + 1$ segments; then m segments end on a branch point (probability Pb_i), but not the last segment (probability $1 - Pb_i$). Thus

$$b_i(m) = Pb_i^m(1 - Pb_i) \tag{7}$$

and for the whole system

$$b(m) = \sum_{i=1}^{q} ps_i b_i(m) \tag{8}$$

Therefore, the number of linear chains (main backbones with no branch points) is

$$n_l = Nb(0) = N\sum_{i=1}^{q} ps_i(1 - Pb_i) \tag{9}$$

whereas the number of main backbones containing at least one branch point reads:

$$n_a = N[1 - b(0)] = N\sum_{i=1}^{q} ps_i Pb_i \tag{10}$$

The number of free arms is then $2n_a$, whereas the number of inner backbones present in the main backbones is given by

$$n_b = N\sum_{m=1}^{\infty}(m - 1)b(m) = N\sum_{i=1}^{q} ps_i \frac{Pb_i^2}{1 - Pb_i} \tag{11}$$

We now start the grafting step. The number of branch points in the system is $N_{BP} = Nn_{BP}$ with

$$n_{BP} = \sum_{m=0}^{\infty} mb(m) = \sum_{i=1}^{q} ps_i \frac{Pb_i}{1 - Pb_i} \tag{12}$$

For each of these branch points, there is a probability

$b(0)$ of grafting a linear chain that will become a free arm, and a probability $1 - b(0)$ of grafting a main backbone containing at least one branch point, thus creating an inner backbone. Thus, the remaining number of linear chains is

$$N_L = n_l - N_{BP}b(0) = n_l - n_{BP}n_l \tag{13}$$

The number of inner backbones after grafting is increased by the number of branched main backbones grafted:

$$N_B = n_b + N_{BP}[1 - b(0)] = n_b + n_{BP}n_a \tag{14}$$

Free arms are created when a linear chain is grafted and consumed when a branched main backbone is grafted. Thus, the number of remaining free arms after grafting is

$$N_A = 2n_a + n_{BP}n_l - n_{BP}n_a \tag{15}$$

The total number of segments is verified by use of eq 16:

$$N_S = N\sum_{m=0}^{\infty}(2m+1)b(m) = N\sum_{i=1}^{q}\frac{ps_i}{1-Pb_i} = n_l + n_b + 2n_a \tag{16}$$

The number fractions of linear chains, free arms, and inner backbones are then obtained by normalizing N_L, N_A, and N_B by N_S.

As segment molecular weights are different for different sites, it is more useful to determine the weight fractions of segments. The weights of various segment types are obtained by introducing segment molecular weights $M_{N,Si}$ in n_l, n_a, and n_b:

$$w_l = N\sum_{i=1}^{q}ps_i(1-Pb_i)M_{N,Si} \tag{17}$$

$$w_a = N\sum_{i=1}^{q}ps_iPb_iM_{N,Si} \tag{18}$$

$$w_b = N\sum_{i=1}^{q}ps_i\frac{Pb_i^2}{1-Pbi}M_{N,Si} \tag{19}$$

and writing the weights of remaining segments as was done in eq 13−15:

$$W_L = w_l - n_{BP}w_l \tag{20}$$

$$W_B = w_b + n_{BP}w_a \tag{21}$$

$$W_A = 2w_a + n_{BP}w_l - n_{BP}w_a \tag{22}$$

The total weight W_S of segments (and also of molecules) is similarly obtained from the expression for N_S:

$$W_S = N\sum_{i=1}^{q}\frac{ps_i}{1-Pb_i}M_{N,Si} \tag{23}$$

Dividing W_L, W_B, and W_A by W_S, we obtain the weight fractions of linear chains, free arms, and inner backbones:

$$\Phi_L = \frac{\left(\sum_{i=1}^{q}\pi_i\frac{\beta_i+1}{2\beta_i+1}\right)\left(\sum_{i=1}^{q}ps_i\frac{1}{\beta_i+1}\right)}{\left(\sum_{i=1}^{q}\pi_i\frac{2\beta_i+1}{\beta_i+1}\right)} \tag{24}$$

$$\Phi_B = \frac{\left(\sum_{i=1}^{q}\pi_i\frac{\beta_i^2}{(\beta_i+1)(2\beta_i+1)}\right) + \left(\sum_{i=1}^{q}ps_i\frac{\beta_i}{\beta_i+1}\right)\left(\sum_{i=1}^{q}\pi_i\frac{\beta_i}{2\beta_i+1}\right)}{\left(\sum_{i=1}^{q}\pi_i\frac{2\beta_i+1}{\beta_i+1}\right)} \tag{25}$$

$$\Phi_A = \frac{2\left(\sum_{i=1}^{q}\pi_i\frac{\beta_i}{2\beta_i+1}\right) + \left(\sum_{i=1}^{q}ps_i\frac{\beta_i}{\beta_i+1}\right)\left(\sum_{i=1}^{q}\pi_i\frac{1}{2\beta_i+1}\right)}{\left(\sum_{i=1}^{q}\pi_i\frac{2\beta_i+1}{\beta_i+1}\right)} \tag{26}$$

where $\pi_i = ps_iM_{N,Si}$.

The total number of molecules N_C is obtained by noting that one main backbone disappears for each branch point created, namely

$$N_C = N[1 - n_{BP}] = N\sum_{i=1}^{q}ps_i\frac{1-2Pb_i}{1-Pb_i} \tag{27}$$

and the average number of branch points per molecule is

$$\bar{\beta} = \frac{N_{BP}}{N_C} = \frac{\sum_{i=1}^{q}ps_i\frac{Pb_i}{1-Pb_i}}{\sum_{i=1}^{q}ps_i\frac{1-2Pb_i}{1-Pb_i}} = \frac{\sum_{i=1}^{q}\frac{ps_i}{\beta_i+1}\beta_i}{\sum_{i=1}^{q}\frac{ps_i}{\beta_i+1}} \tag{28}$$

Then the number-average molecular weight of the system is given by

$$M_N = \frac{W_S}{N_C} = \frac{\sum_{i=1}^{q}\frac{ps_i}{1-Pb_i}M_{N,Si}}{\sum_{i=1}^{q}ps_i\frac{1-2Pb_i}{1-Pb_i}} = \frac{\sum_{i=1}^{q}\frac{ps_i}{\beta_i+1}(2\beta_i+1)M_{N,Si}}{\sum_{i=1}^{q}\frac{ps_i}{\beta_i+1}} \tag{29}$$

Finally, the branching density (number of long chain branchs per 1000C) reads:

$$\lambda = 14\,000\frac{N_{BP}}{W_S} = 14\,000\frac{\bar{\beta}}{M_N} = \frac{14\,000\sum_{i=1}^{q}\frac{ps_i}{\beta_i+1}\beta_i}{\sum_{i=1}^{q}\frac{ps_i}{\beta_i+1}(2\beta_i+1)M_{N,Si}} \tag{30}$$

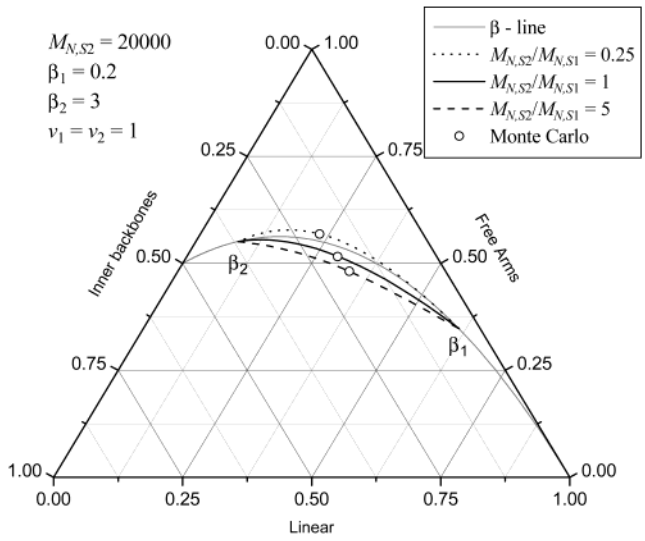

Figure 4. Effect of segment size ratio for a two-LCB-catalyst system with full vinyl termination. β-line refers to locus of composition for a single-site catalyst. The three compositions in Table 1 are represented by a circle.

It can be easily seen that for $q = 1$, all of the previous relations simplify to give the results obtained for the single site system modeled in ref 1.

Figure 4 is an example of the ternary diagram of weight fractions of segments for a mixture of two LCB−CGC catalysts producing only vinyl-terminated molecules. The values of the topological parameter for the catalysts are $\beta_1 = 0.2$ and $\beta_2 = 2.98$; i.e., catalyst 2 produces a very large number of branch points compared to catalyst 1. Note that the value of β_2 is much higher than that of currently available CGC and is chosen for illustrative purposes only. To study the effect of segment size, we choose a number-average segment molecular weight $M_{N,S2} = 20\,000$ and vary $M_{N,S1}$ from $0.2M_{N,S2}$ to $4M_{N,S2}$. The segmental compositions of resins produced by each catalyst fall on the curve representing the locus of possible compositions for a single catalyst ("β-line"), and are denoted β_1 and β_2. The other three curves correspond to the evolution of segmental composition for three values of the ratio $M_{N,S2}/M_{N,S1}$, as predicted by eq 24−26 when the molar fraction ps_2 varies from 0 to 1.

The case $M_{N,S2}/M_{N,S1} = 1$ is interesting, because it is expected to lead to good homogeneity, as all segments in the system have the same MWD. We note that compared to a single catalyst system, it falls below the β-line, which means that one can obtain systems with fewer free arms and more inner backbones, probably leading to a lower viscosity and higher strain hardening. The explanation for this will be given after the derivation of $F_N(n)$, which follows. If the segments from the high branching catalyst are longer ($M_{N,S2}/M_{N,S1} = 5$), the effect is more pronounced, whereas it can be opposite when segments from the low branching catalyst are longer than those from the other catalyst.

Monte Carlo simulations confirmed these results. Detailed data for the three compositions marked by circles in Figure 4 are shown in Table 1. There is very good agreement between model and simulation with 10^5 molecules.

Additional information that can be obtained using this simple model is the number fraction of molecules with

Table 1. Comparison between Monte Carlo Simulation and Model[a] for Complete Vinyl Termination

	MC1	MC2	MC3
$M_{N,S2}/M_{N,S1}$	5	1	0.25
ps_2	0.2	0.45	0.7
pp_1:lp_1	0.9940:0.9990	0.9988:0.9998	0.9997:0.99995
pp_2:lp_2	0.9992:0.9994	0.9992:0.9994	0.9992:0.9994

	MC1		MC2		MC3	
	MC	**model**	MC	**model**	MC	**model**
Φ_L	0.3323	**0.3366**	0.2926	**0.2914**	0.2313	**0.2316**
Φ_A	0.4818	**0.4796**	0.5159	**0.5169**	0.5684	**0.5687**
Φ_B	0.1859	**0.1838**	0.1915	**0.1917**	0.2003	**0.1997**
LCB/10^3C	0.3692	**0.3684**	0.2102	**0.2100**	0.1535	**0.1532**
M_N/28	539.2	**534.2**	1786.1	**1787.1**	4409.9	**4407.3**

[a] $\beta_1 = 0.2$, $\beta_2 = 3$, $M_{N,S2} = 20\,000$, $\nu_1 = \nu_2 = 1$, 1 000 000 molecules.

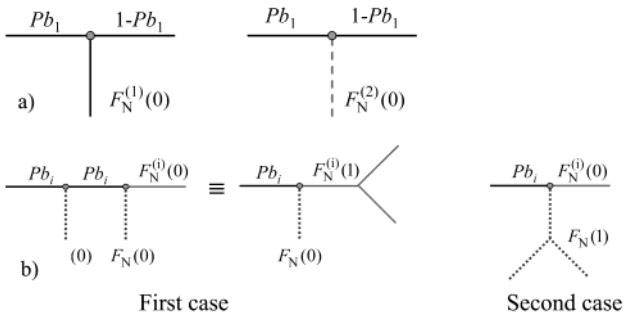

Figure 5. (a) Probabilities of building three-arm stars from catalyst 1. (b) Formation of H-shape molecules from site i.

n branch points, $F_N(n)$. The case of linear chains is trivial:

$$F_N(0) = \frac{N_L}{N_C} = \sum_{i=1}^{q} ps_i F_N^{(i)}(0) \tag{31}$$

where the number fraction of linear chains produced by site i is

$$F_N^{(i)}(0) = 1 - Pb_i \tag{32}$$

This is a direct consequence of the fact that all molecules are vinyl terminated, which means that all the main backbones have the same probability of being grafted as branches. When the number of molecules is reduced by a factor $(1 - N_{BP})$, the number of linear chains is reduced by the same amount, so that the number fraction of linear chains in the branched melt is the same as in the main backbone system.

We now consider molecules with one branch point produced by site i, as shown in Figure 5a for the simple case $q = 2$. The first segment, finishing on a branch point, has a probability Pb_i, and the second segment has a probability $(1 - Pb_i)$, i.e. $F_N^{(i)}(0)$. The branch is a linear chain produced by any site, with a probability $F_N(0)$. Then we can write the probability of finding a molecule with one branch point produced by site i as

$$F_N^{(i)}(1) = Pb_i F_N(0) F_N^{(i)}(0) \tag{33}$$

Summing over all the sites gives the number fraction of molecules with one branch point:

$$F_N(1) = \sum_{i=1}^{q} ps_i F_N^{(i)}(1) \quad (34)$$

For a molecule with two branch points produced by site *i*, we have to consider two cases, as pictured in Figure 5b. The first case concerns main backbones with two branch points, on which two linear chains are grafted. If the main backbone is produced by site *i*, the first segment has a probability Pb_i, and the first branch a probability $F_N(0)$, since it is a linear chain made by any site. The rest of the molecule is then a three-arm star produced by site *i*, with a probability $F_N^{(i)}(1)$. In the second case, we graft a three-arm star made by any site onto a main backbone with one branch point produced by site *i*. In this case, the first segment has a probability Pb_i, the branch a probability $F_N(1)$, and the last segment a probability $1 - Pb_i = F_N^{(i)}(0)$.

We can then write

$$F_N^{(i)}(2) = Pb_i F_N(0) F_N^{(i)}(1) + Pb_i F_N(1) F_N^{(i)}(0) \quad (35)$$

Thus, for all molecules with two branch points, the number fraction is

$$F_N(2) = \sum_{i=1}^{q} ps_i F_N^{(i)}(2) \quad (36)$$

This can be easily generalized, in a recurrence process similar to the one used to obtain the relation giving the Catalan numbers in ref 1. For molecules with *n* branch points, the number fraction is given by

$$F_N(n) = \sum_{i=1}^{q} ps_i F_N^{(i)}(n) \quad (37)$$

and

$$F_N^{(i)}(n) = Pb_i \sum_{k=0}^{n-1} F_N(k) F_N^{(i)}(n-k-1) \quad (38)$$

The weight fractions can also be obtained, but as the derivation is somewhat tedious, we postpone it to the more general case of incomplete vinyl termination.

Figure 6 shows a comparison of Monte Carlo results with eq 37 for the set MC2 of Table 1. As for this set all segments have the same molecular weight distribution, segmental weight fractions are equal to number fractions. To explain why MC2 falls below the β-line on the ternary diagram, we plot the ratio of $F_N(n)$ to the number fraction of molecules with *n* branch points, $\bar{F}_N(n)$, for a single catalyst resin[1,7] having the same average number of branch points per molecule, $\bar{\beta}$, given by eq 28. We call this ratio $R_N(n)$:

$$R_N(n) = \frac{F_N(n)}{\bar{F}_N(n)} \quad \text{with} \quad \bar{F}_N(n) = \frac{(2n)!}{n!(n+1)!} \frac{\bar{\beta}^n (\bar{\beta}+1)^{n+1}}{(2\bar{\beta}+1)^{2n+1}} \quad (39)$$

It can be seen that for *n* between 2 and 6, $R_N(n)$ is less than one, but is larger than one for linear chains and for molecules with more than seven branch points. As a molecule with *n* branch points possesses $n + 2$ free arms for $n - 1$ inner backbones, decreasing the number of molecules with a few branch points increases the ratio of inner backbones to free arms. It also contributes to an increase in the average seniority of inner backbones, which should impact strain hardening favorably.

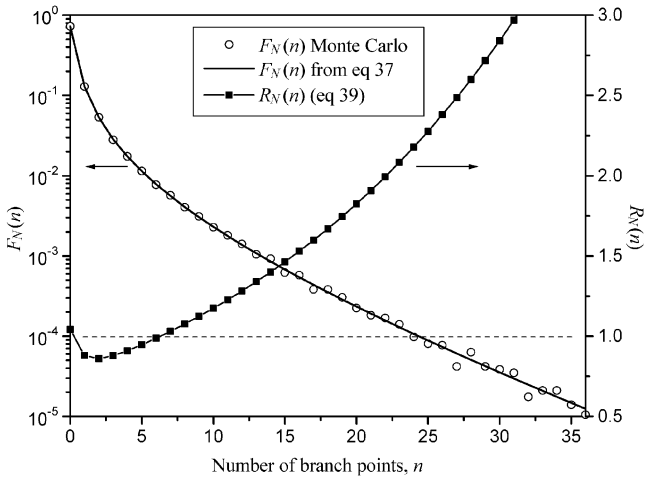

Figure 6. Variation of number fraction of molecules with *n* branch points in the case of complete vinyl termination (from eq 37) and Monte Carlo simulation.

Real Situation: Partial Vinyl Termination

The above result can be adapted to the case where the rate of vinyl termination is different for each site. The effect of vinyl termination is complex, because it is 2-fold. First, it will affect the probability that molecules produced by a given site can be used as macromonomers. This is a simple mixing effect, which is the object of the following section. Second, as the overall concentration of macromonomer depends on the rates of vinyl termination of the various catalysts and on the composition, the rates of long chain branching for each catalyst will change when it is mixed with others. This effect will be analyzed later.

We assume that for site *i*, a fraction v_i of main backbones will be vinyl terminated, whereas the fraction of dead chains is $(1 - v_i)$. The values of Pb_i, β_i and $M_{N,Si}$ are those of catalyst *i* when it is mixed with others, and they therefore correspond to a given composition and a given set of vinyl-termination probabilities.

The expressions for n_l, n_a, and n_b are still given by eqs 9−11, but we can now split n_l and n_a into two terms each, with superscripts = and + for vinyl-terminated and dead (saturated) main backbones respectively:

$$n_l = n_l^{=} + n_l^{+} \quad \text{with} \quad n_l^{=} = N \sum_{i=1}^{q} ps_i v_i (1 - Pb_i) \quad (40)$$

and

$$n_a = n_a^{=} + n_a^{+} \quad \text{with} \quad n_a^{=} = N \sum_{i=1}^{q} ps_i v_i Pb_i \quad (41)$$

The total number of main backbones terminated by a vinyl group is

$$n^{=} = n_l^{=} + n_a^{=} = N \sum_{i=1}^{q} ps_i v_i \quad (42)$$

Repeating the same process as before, we obtain the number of linear chains, free arms, and inner back-

bone when vinyl termination is incomplete:

$$\check{N}_L = n_l - N_{BP}\frac{n_l^=}{n^=} \tag{43}$$

$$\check{N}_B = n_b + N_{BP}\frac{n_a^=}{n^=} \tag{44}$$

$$\check{N}_A = 2n_a - N_{BP}\frac{n_a^=}{n^=} + N_{BP}\frac{n_l^=}{n^=} \tag{45}$$

In the following, the symbol ˇ on a variable indicates a general expression for partial vinyl termination. The value $n^=$ is introduced to take into account the fact that segments to be grafted have to be chosen among vinyl-terminated main backbones only. The total number of segments, N_S, and the number of molecules remaining, N_C, are still given by eqs 16 and 27.

We note that in order to have full branching, the number of vinyl terminated segments must be sufficient to fill all the BP, so the following condition must be satisfied:

$$\sum_{i=1}^{q} ps_i \nu_i > n_{BP} \tag{46}$$

This condition is an artifact of the Monte Carlo method, as will be explained later.

The weight fractions of segments are also affected by the introduction of vinyl termination. Using the same principle as before, the weights of each type of segment are obtained:

$$\check{W}_L = w_l - \frac{N_{BP}}{n^=} w_l^= \tag{47}$$

$$\check{W}_B = w_b + \frac{N_{BP}}{n^=} w_a^= \tag{48}$$

$$\check{W}_A = 2w_a - \frac{N_{BP}}{n^=} w_a^= + \frac{N_{BP}}{n^=} w_l^= \tag{49}$$

where

$$w_l^= = N\sum_{i=1}^{q} ps_i \nu_i (1 - Pb_i) M_{N,Si} \tag{50}$$

and

$$w_a^= = N\sum_{i=1}^{q} ps_i \nu_i Pb_i M_{N,Si} \tag{51}$$

The total weight W_S is unchanged from eq 23, which means that M_N and $\bar{\beta}$ (and consequently the branching density) are independent of vinyl termination when β_i (or Pb_i), $M_{N,Si}$, and ps_i are fixed.

The weight fractions of linear, inner backbones, and free arms are obtained by dividing $\check{W}_L$, $\check{W}_A$, and $\check{W}_B$ by the total weight W_S to give

$$\check{\Phi}_L = \frac{\left(\sum_{i=1}^{q} \pi_i \frac{\beta_i + 1}{2\beta_i + 1}\right) - \left(\sum_{i=1}^{q} ps_i \frac{\beta_i}{\beta_i + 1}\right)\left(\sum_{i=1}^{q} \rho_i \frac{\beta_i + 1}{2\beta_i + 1}\right)}{\left(\sum_{i=1}^{q} \pi_i \frac{2\beta_i + 1}{\beta_i + 1}\right)} \tag{52}$$

$$\check{\Phi}_B = \frac{\left(\sum_{i=1}^{q} \pi_i \frac{\beta_i^2}{(\beta_i + 1)(2\beta_i + 1)}\right) + \left(\sum_{i=1}^{q} ps_i \frac{\beta_i}{\beta_i + 1}\right)\left(\sum_{i=1}^{q} \rho_i \frac{\beta_i}{2\beta_i + 1}\right)}{\left(\sum_{i=1}^{q} \pi_i \frac{2\beta_i + 1}{\beta_i + 1}\right)} \tag{53}$$

$$\check{\Phi}_A = \frac{2\left(\sum_{i=1}^{q} \pi_i \frac{\beta_i}{2\beta_i + 1}\right) + \left(\sum_{i=1}^{q} ps_i \frac{\beta_i}{\beta_i + 1}\right)\left(\sum_{i=1}^{q} \rho_i \frac{1}{2\beta_i + 1}\right)}{\left(\sum_{i=1}^{q} \pi_i \frac{2\beta_i + 1}{\beta_i + 1}\right)} \tag{54}$$

where $\pi_i = ps_i M_{N,Si}$ and

$$\rho_i = \frac{ps_i \nu_i}{\sum_{i=1}^{q} ps_i \nu_i} M_{N,Si} \tag{55}$$

We note that for a single-site ($q = 1$) characterized by β, $M_{N,S}$, and ν, the parameters ν and $M_{N,S}$ disappear, and the fractions simplify to eqs 8 and 9 of ref 1.

Number and weight-average molecular weights of linear chains, inner backbones, and free arms in the case of partial vinyl termination are

$$\check{M}_{NL} = \frac{\check{W}_L}{\check{N}_L} \quad \check{M}_{NB} = \frac{\check{W}_B}{\check{N}_B} \quad \check{M}_{NA} = \frac{\check{W}_A}{\check{N}_A} \tag{56}$$

$$\check{M}_{WL} = \frac{\check{Z}_L}{\check{W}_L} \quad \check{M}_{WB} = \frac{\check{Z}_B}{\check{W}_B} \quad \check{M}_{WA} = \frac{\check{Z}_A}{\check{W}_A} \tag{57}$$

The second moments $\check{Z}_\alpha$ are built on the model of the first moments $\check{W}_\alpha$

$$\check{Z}_L = z_l - \frac{N_{BP}}{n^=} z_l^= \tag{58}$$

$$\check{Z}_B = z_b + \frac{N_{BP}}{n^=} z_a^= \tag{59}$$

$$\check{Z}_A = 2z_a - \frac{N_{BP}}{n^=} z_a^= + \frac{N_{BP}}{n^=} z_l^= \tag{60}$$

where the z terms are computed similarly to the corresponding w term by replacing in eqs 17−19, 50, and 51 the weight $M_{N,Si}$ by $M_{N,Si}M_{W,Si} = 2M_{N,Si}^2$.

Figure 7 shows the first effect of partial vinyl termination for a two-catalyst system. We keep all parameters of the fully vinyl-terminated system MC1 (see

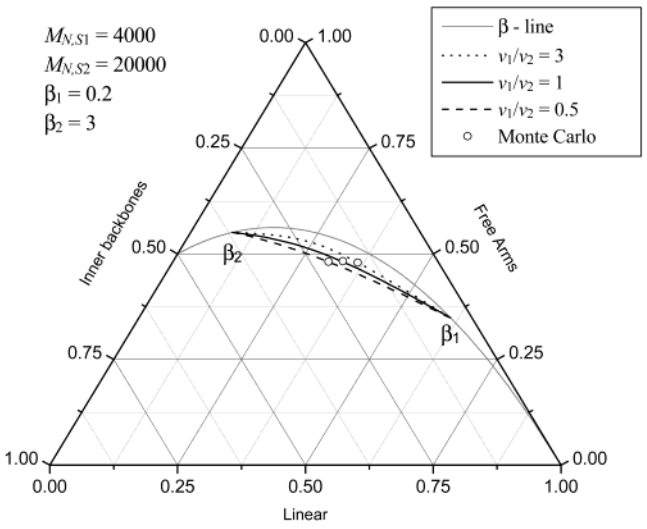

Figure 7. Evolution of segmental composition with ratio of vinyl-termination probabilities. Monte Carlo simulation data are reported in Table 2.

Table 1) but alter the vinyl-termination probability, so that $\nu_1/\nu_2 = 0.5$, 1, and 3. The agreement between Monte Carlo and model, shown in Table 2, is excellent. Note that system MC1b gives results identical to MC1, since only the ratio ν_1/ν_2 affects the structure. We conclude from Figure 7 that the independent effect of mixing catalysts (keeping β_i and $M_{N,Si}$ constant for all compositions) is favorable when ν_1/ν_2 is less than 1. In this case, molecules from highly branching catalyst 2 are more likely to be used as branches than those produced by the catalyst with low β, leading to many hyperbranched molecules which contribute to fewer free arms than smaller molecules. On the other hand, when ν_1/ν_2 is larger than 1, branches from catalyst 1 are more numerous and as β_1 is low, a large fraction of these branches will be linear. This will lead to more free arms than the other situation, but we expect the fraction of comb molecules to be larger.

We now compute the fractions of molecules with n branch points, starting with linear chains. The number fraction of linear chains after branching is given by

$$\check{F}_N(0) = \frac{\check{N}_L}{N_C} = \frac{n_l - N_{BP} n_l^{=}/n^{=}}{N(1 - n_{BP})} \tag{61}$$

Taking into account the definitions of n_l and $n_l^{=}$, we obtain

$$\check{F}_N(0) = \sum_{i=1}^{q} ps_i b_i \check{F}_N^{(i)}(0) \tag{62}$$

where

$$\check{F}_N^{(i)}(0) = 1 - Pb_i \tag{63}$$

is simply the probability that site i makes a main backbone with no branch points. We introduce two new coefficients:

$$a_i = \frac{\nu_i}{n^{=}/N} = \frac{\nu_i}{\sum_{i=1}^{q} ps_i \nu_i} \tag{64}$$

$$b_i = \frac{1 - a_i n_{BP}}{1 - n_{BP}} \tag{65}$$

where a_i is the effective vinyl-termination probability, illustrating the fact that if we multiply every ν_i by the same constant, the topology is not modified. This is in agreement with the results of Beigzadeh et al.,[14,15] who showed that for a two-catalyst system, structural properties can be expressed as functions of the ratio ν_1/ν_2. The parameter b_i appears as a reactivity probability, accounting for the fact that during the branching process a fraction n_{BP} of the main backbones is consumed, but only a fraction $a_i n_{BP}$ of molecules from site i are used as branches. We note that a_i and b_i satisfy the relations

$$\sum_{i=1}^{q} ps_i a_i = 1 \qquad \sum_{i=1}^{q} ps_i b_i = 1 \tag{66}$$

In the special case where all the sites have the same vinyl probability, a_i and b_i are equal to 1, as was explained in the comment following eq 32.

Another useful parameter is the number fraction of vinyl-terminated linear chains:

$$\check{F}_N^{=}(0) = \frac{\sum_{i=1}^{q} ps_i \nu_i (1 - Pb_i)}{\sum_{i=1}^{q} ps_i \nu_i} = \sum_{i=1}^{q} ps_i a_i \check{F}_N^{(i)}(0) \tag{67}$$

To get the number fractions of molecules containing n branch points, we use the same recurrent process as in the case where all molecules are vinyl terminated, but with a crucial difference. In eq 38, the term $F_N(k)$ corresponds to the probability of grafting a branch containing k branch points. In the present case, a branch with k branch points can be grafted only if it is vinyl terminated, and this term therefore has to be replaced by $\check{F}_N^{=}(k)$. The recurrence then reads:

$$\check{F}_N^{(i)}(n) = Pb_i \sum_{k=0}^{n-1} \check{F}_N^{=}(k) \check{F}_N^{(i)}(n - k - 1) \tag{68}$$

$$\check{F}_N(n) = \sum_{i=1}^{q} ps_i b_i \check{F}_N^{(i)}(n) \tag{69}$$

$$\check{F}_N^{=}(n) = \sum_{i=1}^{q} ps_i a_i \check{F}_N^{(i)}(n) \tag{70}$$

We can similarly obtain the weight fractions by introducing the weights, $\check{W}(n)$, $\check{W}^{=}(n)$ and $\check{W}^{(i)}(n)$, respectively, of molecules with nBP, vinyl-terminated molecules containing nBP, and molecules with nBP made by site i:

Table 2. Comparison between Monte Carlo Simulation[a] and Model[b] for Partial Vinyl Termination

	MC1a v_1:v_2 = 0.5:1		MC1b v_1:v_2 = 0.75:0.75		MC1c v_1:v_2 = 0.9:0.3	
	MC	model	MC	model	MC	model
Φ_L	0.3047	0.3085	0.3321	0.3366	0.3627	0.3625
Φ_A	0.4815	0.4796	0.4825	0.4796	0.4796	0.4796
Φ_B	0.2138	0.2119	0.1854	0.1838	0.1577	0.1579
LCB/10^{3}C	0.3692	0.3684	0.3692	0.3684	0.3669	0.3684
M_N/28	539.1	534.2	539.1	534.2	535.0	534.2

[a] $pp_1 = 0.994$, $lp_1 = 0.9990$, $pp_2 = 0.9992$, $lp_2 = 0.9994$, $ps_2 = 0.2$, 1 000 000 molecules. [b] $\beta_1 = 0.2$, $\beta_2 = 3$, $M_{n,S2} = 20\,000$, $M_{n,S1} = 4000$, $ps_2 = 0.2$.

$$\check{W}(n) = \sum_{i=1}^{q} ps_i b_i \check{W}^{(i)}(n) \tag{71}$$

$$\check{W}^{=}(n) = \sum_{i=1}^{q} ps_i a_i \check{W}^{(i)}(n) \tag{72}$$

$$\check{W}^{(i)}(n) = Pb_i \sum_{k=0}^{n-1} \check{F}_N^{=}(k) \check{F}_N^{(i)}(n-k-1)[\check{M}_N^{(i)}(0) + \check{M}_N^{=}(k) + \check{M}_N^{(i)}(n-k-1)] \tag{73}$$

where the factor between brackets represent the number-average molecular weight of a molecule formed by one segment from site i, one branch with k branch points, and one molecule from site i with $(n - k - 1)$ branch points as explained before.

To determine $\check{W}^{(i)}(n)$, we need the number-average molecular weights $\check{M}_N^{=}(j)$ and $\check{M}_N^{(i)}(j)$, respectively, of vinyl-terminated molecules containing j branch points and molecules with j branch points made by site i, for all $j < n$. This can easily be obtained in the recurrence process according to the following relations:

$$\check{M}_N^{=}(j) = \frac{\check{W}^{=}(j)}{\check{F}_N^{=}(j)} \tag{74}$$

$$\check{M}_N^{(i)}(j) = \frac{\check{W}^{(i)}(j)}{\check{F}_N^{(i)}(j)} \tag{75}$$

The recurrence is started by noting that

$$\check{M}_N^{(i)}(0) = M_{N,Si} \tag{76}$$

$$\check{W}^{(i)}(0) = \check{F}_N^{(i)}(0) M_{N,Si} \tag{77}$$

from which $\check{W}(0)$ and $\check{W}^{=}(0)$ can be obtained using eqs 71 and 72. Finally, the weight fraction of molecules with n branch points is obtained by dividing $\check{W}(n)$ by the number-average molecular weight of all molecules given by eq 29:

$$\check{F}_W(n) = \frac{\check{W}(n)}{M_N} \tag{78}$$

The number-average molecular weight of molecules with n branch points is

$$\check{M}_N(n) = \frac{\check{W}(n)}{\check{F}_N(n)} \tag{79}$$

The weight-average molecular weight of molecules with n branch points and of the whole system can also be determined, as explained in Appendix A.

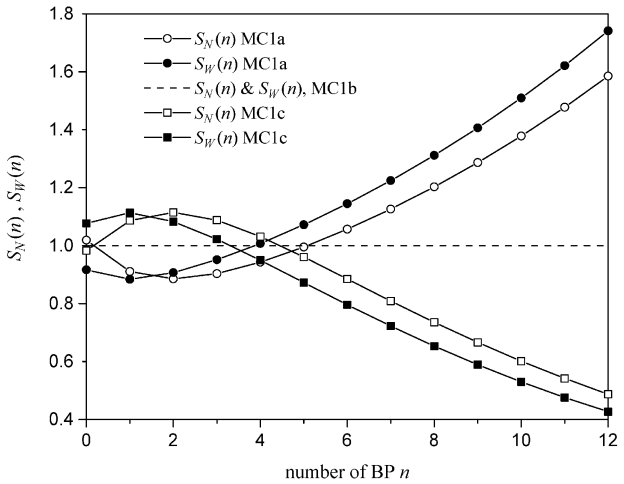

Figure 8. Ratio of number and weight fractions of molecules with nBP for several vinyl terminations (MC1a, MC1b, and MC1c from Table 2), to the same quantity for complete vinyl termination (MC1 from Table 1).

These results confirm the explanation given above of the results shown in Figure 7. As $\bar{\beta}$ for MC1a, MC1b, and MC1c is the same as for MC1 (we see in Table 2 that the values of LCB/1000C and M_N are identical), instead of $R_N(n)$ from eq 39, we compare the ratio of $\check{F}_N(n)$for each system in Table 2 to $F_N(n)$ for MC1. This ratio, denoted $S_N(n)$, corresponds to the independent effect of vinyl termination on the frequency of molecules with nBP. The results are displayed in Figure 8, together with the ratios of weight fractions, $S_W(n)$. As only the ratio v_1/v_2 affects $\check{F}_N(n)$, system MC1b gives the same result as MC1, leading to ratios $S_N(n)$ and $S_W(n)$ of 1. System MC1a gives a ratio smaller than one for small values of n, but larger than 1 for $n > 5$, whereas the behavior is the opposite for MC1c. This confirms that when the catalyst having a high β in the mixture has more vinyl terminations than the other catalyst, the effect of mixing the two sites is to create more hyperbranched molecules than if the vinyl-termination probabilities are equal. Before any conclusion can be drawn regarding optimization of combined systems, we need to include the second effect of vinyl termination.

Effect of Overall Concentration of Macromonomers

In the model presented above we took pp_i and lp_i to be the probabilities for catalyst i in the reactor, in the presence of all the other catalysts. These values are not accessible experimentally, but can be obtained when catalyst i is used alone. Nevertheless, when we mix the catalysts together, the concentration of macromonomers is not the same as for the catalyst alone (except if all the catalysts have the same vinyl-termination prob-

ability v_i), and the monomer selection probability is altered. Provided that experimental conditions be kept the same, the propagation probability can be considered to be identical in the mixture of catalysts as for the catalyst alone.

The model takes into account the macromonomer concentration in the mixture through the parameter a_i. From characterization by NMR or LALLS of a material produced from catalyst i alone, we can determine the value of the vinyl-termination probability v_i, and of the monomer selection probability lp_i^*. In the catalyst mixture, the vinyl-termination probability becomes $\sum_j \mathrm{ps}_j \nu_j$, and the new value lp_i of the monomer selection probability remains to be assessed. This can be done easily by introducing $\mathrm{lp}_i^{(0)}$, the value of the monomer selection probability that the catalyst alone would have under conditions of complete vinyl termination, where it can provide its maximum branching density. The probability lp_i^* can be related to $\mathrm{lp}_i^{(0)}$ by[1]

$$\mathrm{lp}_i^* = \frac{\mathrm{lp}_i^{(0)}}{\mathrm{lp}_i^{(0)} + v_i(1 - \mathrm{lp}_i^{(0)})} \tag{80}$$

Then when the catalyst is in a mixture of average vinyl termination $\sum_j \mathrm{ps}_j \nu_j$, the monomer selection probability becomes

$$\mathrm{lp}_i = \frac{\mathrm{lp}_i^{(0)}}{\mathrm{lp}_i^{(0)} + \sum_j \mathrm{ps}_j \nu_j (1 - \mathrm{lp}_i^{(0)})} \tag{81}$$

Eliminating $\mathrm{lp}_i^{(0)}$ and using eq 64, we obtain

$$\mathrm{lp}_i = \frac{\mathrm{lp}_i^*}{\mathrm{lp}_i^* + a_i^{-1}(1 - \mathrm{lp}_i^*)} \tag{82}$$

We note that $a_i = 0$ implies that this catalyst alone is unable to create macromonomers and is therefore a linear-CGC. As a consequence, both lp_i^* and lp_i are equal to 1.

In summary, if characterization under given reactor conditions provides for single catalyst i the parameters β_i^* , $M_{\mathrm{N,S}i}^*$, and v_i, the probabilities pp_i^* and lp_i^* can be obtained from

$$\mathrm{pp}_i^* = \frac{(2\beta_i^* + 1)(M_{\mathrm{N,S}i}^*/28 - 1) + \beta_i^*}{(2\beta_i^* + 1)(M_{\mathrm{N,S}i}^*/28)} \tag{83}$$

$$\mathrm{lp}_i^* = \frac{(2\beta_i^* + 1)(M_{\mathrm{N,S}i}^*/28 - 1)}{(2\beta_i^* + 1)(M_{\mathrm{N,S}i}^*/28 - 1) + \beta_i^*} \tag{84}$$

When mixing this catalyst with others, keeping the same reactor conditions, $\mathrm{pp}_i = \mathrm{pp}_i^*$ and lp_i is given by eq 82. The value of β_i and $M_{\mathrm{N,S}i}$ to be used in the model are then obtained from pp_i and lp_i, using eq 1 and 2.

Note that if $1\text{-}\mathrm{lp}_i^*$ is much smaller than lp_i^*, eq 82 can be approximated by

$$\mathrm{lp}_i \cong 1 - a_i^{-1}(1 - \mathrm{lp}_i^*) \tag{85}$$

with a very small error if $M_{\mathrm{N,S}i}^*/28 \gg 1$.

In this case the following simple expressions provides an excellent approximation:

$$\beta_i \cong \frac{\beta_i^*}{(\beta_i^* + 1)a_i - \beta_i^*} \tag{86}$$

$$M_{\mathrm{N,S}i} \cong \frac{(2\beta_i^* + 1)a_i M_{\mathrm{N,S}i}^*}{(\beta_i^* + 1)a_i + \beta_i^*} \tag{87}$$

Comparison with Reaction Kinetics Modeling

Beigzadeh et al.[14,21] proposed an expression for the branching density λ for a combination of a linear-CGC and a LCB−CGC. The LCB per 1000 carbon atoms as a function of kinetic constants and concentration is

$$\lambda = 500\frac{\lfloor(k_{\beta 2} + k_{\mathrm{fm}2}M) - (k_{\beta 1} + k_{\mathrm{fm}1}M)\rfloor r + k_{\beta 1} + k_{\mathrm{fm}1}M}{M[(k_{p2} - k_{p1})r + k_{p1}]} \times \left[1 - \frac{1 - \exp(-k_{\mathrm{LCB}}Crt)}{k_{\mathrm{LCB}}Crt}\right] \tag{88}$$

where C is the total catalyst concentration, r is the fraction of CGC in the reactor, M is the monomer concentration, t is the polymerization time, and k_β, k_{fm}, k_{p}, and k_{LCB} are the rate constants for β-hydride elimination, transfer to monomer, propagation, and LCB incorporation, respectively. In eq 88, subscripts 1 and 2 refer respectively to the linear-CGC and the LCB−CGC. The parameter values given in ref 14 are as follows: $k_{\mathrm{p}1} = k_{\mathrm{p}2} = 4000$ L/mol·s, $k_{\mathrm{LCB}} = 600$ L/mol·s, $C = 4$ μmol/L, $M = 0.9$ mol/L, and $t = 600$ s. Terms $k_\beta + k_{\mathrm{fm}}M$ correspond to rates of macromonomer formation. The value is $k_{\beta 2} + k_{\mathrm{fm}2}M = 0.1\ \mathrm{s}^{-1}$ for LCB−CGC, and five values are taken for the linear catalyst so that $(k_{\beta 1} + k_{\mathrm{fm}1}M)/(k_{\beta 2} + k_{\mathrm{fm}2}M)$ is 0.5, 1, 2, 3, and 5. The variation of λ with mole fraction of LCB−CGC is shown in Figure 9 as continuous curves.[22]

To apply the present model to this particular case, we need the topological and dimensional parameters for catalysts 1 and 2. As already mentioned, only the ratio of vinyl-termination probabilities is important in a two-catalyst system, so we can choose any values of v_1 and v_2 such that the ratio v_1/v_2 takes the values 0.5, 1, 2, 3, and 5. Then the branching density when catalyst 2 is used alone should be equal to the value given by eq 88 when $r = 1$, namely $\lambda_2^* = 6.53 \times 10^{-3}$ LCB/1000C. The values of β_2^* and $M_{\mathrm{N,S2}}^*$ can be chosen freely, provided that we satisfy the following relation:

$$\lambda_2^* = 14\,000\frac{\beta_2^*}{(2\beta_2^* + 1)M_{\mathrm{N,S2}}^*} = 14\,000\frac{Pb_2^*}{M_{\mathrm{N,S2}}^*} \tag{89}$$

We choose for instance $M_{\mathrm{N,S2}}^* = 30\,000$, which leads to $\beta_2^* = 0.0144$. As the other site makes linear chains only, $\beta_1^* = 0$, and the only parameter left is $M_{\mathrm{N,S1}}^*$. We use $M_{\mathrm{N,S2}}^*/M_{\mathrm{N,S1}}^* = 1.545$ as the (only) fitting parameter, and we compute $M_{\mathrm{N,S1}}$, β_2, and $M_{\mathrm{N,S2}}$ from eq 86 and 87. The branching density is obtained from eq 30 and we obtain excellent agreement for all five curves, as shown in Figure 9. This illustrates the fact that the model requires the minimal number of parameters to predict the branching density of linear-/LCB−CGC systems, namely the ratio of number-average MW of segments from LCB−CGC to that from linear-CGC, the branching density for LCB−CGC when it is used alone in the same reactor conditions and the ratio of vinyl-

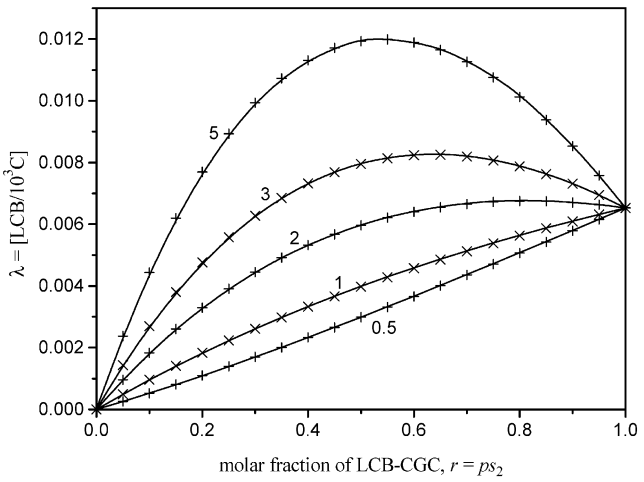

Figure 9. Comparison of present model (symbols) with results of Beigzadeh et al.(lines) for five values of ν_1/ν_2. Parameters are given in the text.

termination probabilities of linear-CGC to LCB−CGC. The polymerization time does not appear explicitely because it is a constant in Figure 9. In this case, Monte Carlo-based models and the method of balance of moments are equivalent to predict average properties such as LCB density.

Molecular Weight Distribution

The last aspect of the branched system statistics to be calculated is the molecular weight distribution (MWD). In the case of branched systems, it is not possible to determine experimentally the true MWD by GPC due to the nature of the separation process, the molecules being eluted according to their hydrodynamic volume and not their molecular weight. The use of triple-detector GPC, and of approximations derived from the classical theory of Zimm and Stockmayer lead to fairly good results in the case of polymers made with a single-site CGC catalyst, but the approximations fail for different statistics of branching. No evidence of the validity of this technique for multiple CGC−catalysts systems has been published yet, and modeling of the true MWD is useful in this respect as well as for optimization of processability. Derivation of an exact solution is a very tedious task, and instead we propose in Appendix B an approximate solution that may be sufficient for property optimization purposes. By construction, this MWD has the correct number and weight-average molecular weights. Since we compute the exact MWD of linear chains and three-arm stars, we expect the approximate MW to be quite accurate in the low molecular weight range. The high molecular weight tail should also be correctly estimated as explained in Appendix B. This leaves an interval of about one decade of molecular weight where details of the actual MWD cannot always be accurately predicted by the model.

Optimization of BmPE Properties

The first step in optimizing the processing properties of a resin is to establish criteria for the resin in terms of homogeneity, viscosity or flow rate, and strain hardening. Quantitative prediction of rheological properties is not easy, due to the difficulty in correlating viscoelastic properties with parameters such as segment size and polydispersity, segmental composition, fraction of molecules with n branch points or seniority distribution,[7] which cannot be measured experimentally. Advanced tube models usually deal with monodisperse stars[4] or combs,[5] and they cannot predict quantitatively the aforementioned properties because of the complexity of the stress relaxation mechanisms involved. We therefore use simplified criteria to compare resins by considering only weight-average MW and weight fractions of linear chains, free arms, and inner backbone segments.

A typical case of optimization of processability is to maximize extensional strain hardening, or "melt strength" without increasing the shear viscosity. For single-site catalyst resins, increasing strain hardening is usually accompanied by a significant increase of the zero-shear viscosity. Linear chains contribute to viscosity, but to a small extent compared to free arms, for which the dependence on arm size and fraction is roughly exponential[23,24] Linear molecules also act as a diluent for the other segments, because reptation of linear species accelerates the relaxation of free arms by a Rouse-like constraint release mechanism. Free arms contribute strongly not only to viscosity but also to strain hardening when they are part of a molecule containing inner backbones. In this respect, three-arm stars should be minimized since they only increase the viscosity. Unfortunately, the weight fraction of molecules with n branch points, $\check{F}_W(n)$, is always a monotonic decreasing function, and the weight fraction of stars is consequently always larger than the fraction of more complex molecules. Decreasing the fraction of free arms compared to inner backbones can only be accomplished by increasing the fraction of highly branched molecules compared to molecules with a few branch points, as was shown by the ratio $R_N(n)$. This can be achieved by combining at least two CGC catalyst, by optimizing the mole fraction of each catalyst, their propensity to incorporate long-chain branches and to create unsaturated molecules, which is affected by the reactor conditions.

Combinations of catalysts will usually yield a larger polydispersity than a single catalyst. This is not necessarily a drawback for processing, as it is well-known that introducing high molecular weight material can aid the processing of metallocene PE by increasing its shear-thinning tendency.

The ternary diagram will now be used to compare resins, and we limit ourselves to a combination of a linear catalyst and a LCB catalyst. First we will study the linear/LCB system of Figure 9. As the level of branching is extremely low, we rescale all the curves of Figure 9 vertically by setting $\beta_2^* = 0.4$, keeping $M_{N,S2}^* = 30\,000$. The value of ν_2 must be chosen to satisfy the condition[1]

$$\nu_2 > \frac{\beta_2^*}{1+\beta_2^*} \tag{90}$$

to ensure that the resin characterized by β_2^*, $M_{N,S2}^*$, and ν_2 can be synthesized. Since the maximum value for ν_1 is 1, the maximum value of ν_1/ν_2 that can be achieved will be

$$[\nu_1/\nu_2]_{max} = \frac{1+\beta_2^*}{\beta_2^*} \tag{91}$$

which, for $\beta_2^* = 0.4$ gives $\nu_1/\nu_2 < 3.5$.

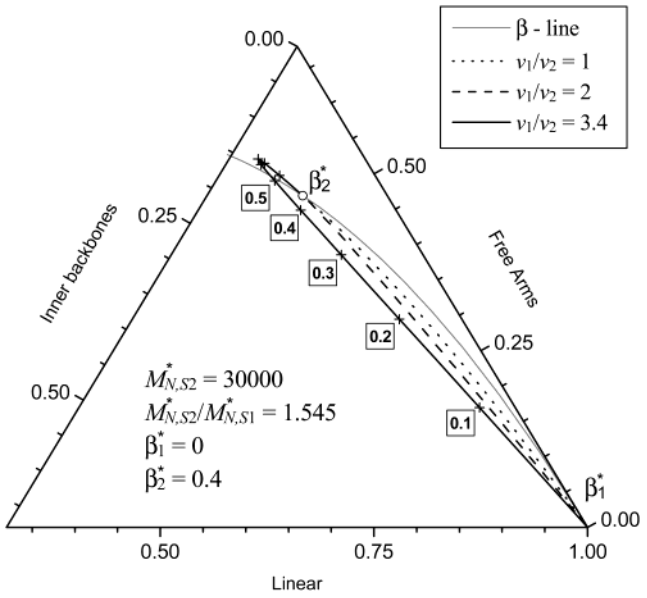

Figure 10. Full model prediction of the ternary diagram of segmental composition for a mixture of two catalysts for different vinyl termination ratio v_1/v_2. Values of ps_2 are labeled for the maximum ratio.

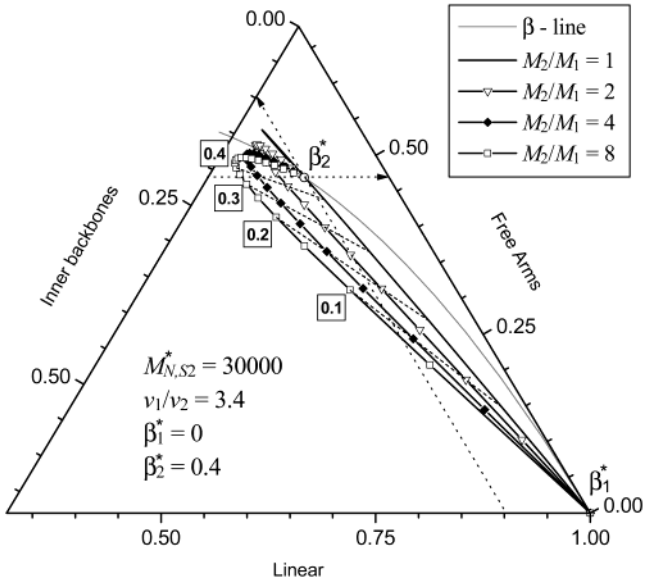

Figure 11. Full model prediction of the ternary diagram of segmental composition for a mixture of two catalysts for different initial segment size ratio. M_i refers to $M^*_{N,Si}$. Dashed lines correspond to constant molar fraction ps_2 indicated by the labels. Dotted arrows indicate the fraction of inner backbones and free arms at point β_2^*.

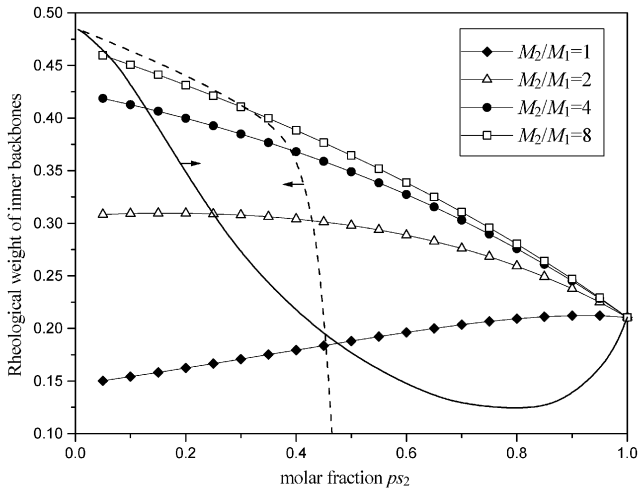

Figure 12. Relative weight of inner backbones to free arms for the systems of Figure 11. The domain indicated by the arrows correspond higher fraction of inner backbones and lower fractions of free arms than at point β_2^* on the ternary diagram.

Figure 10 shows a portion of the ternary diagram for three values of v_1/v_2: 1, 2, and 3.4. Only for $v_1/v_2 = 3.4$ is there a relative increase of the inner backbone fraction. We note that, above $ps_2 = 0.5$, the curve passes above the β-line, indicating a worsening of properties. The criterion $ps_2 = 0.5$, recommended by Beigzadeh for maximum LCB/1000C, actually leads to a segmental composition very close to what would be achieved with a single catalyst. Lower values of ps_2 provide more interesting compromises to optimize the ratio of inner backbones to free arms. The conclusion that segments of the LCB−CGC with higher β* must have less vinyl termination that those of the linear-CGC (or LCB−CGC with lower β*) is contrary to the results shown in Figure 7. This means that the second effect of vinyl termination, i.e., the modification of branching probabilities when mixing the catalysts, is the dominant effect in the optimization process.

Keeping the largest value for v_1/v_2, and setting $M^*_{N,S2} = 30\,000$, we now study the influence of the molecular weight of segments for the linear catalyst. The ratio $M^*_{N,S2}/M^*_{N,S1}$ is varied between 1 and 8, and the impact on the ternary diagram is shown in Figure 11. For $M^*_{N,S2}/M^*_{N,S1} = 1$ we note that the compositions are close to the tie line joining points β_1^* and β_2^*, which is the locus of all blends obtained by mixing materials produced by each catalyst.[1] When the ratio is increased, it becomes possible to achieve compositions below the tie line, and so for every composition when the ratio is 2 or larger. The values of ps_2 above which the fraction of inner backbones becomes larger than at β_2^* are respectively 0.25, 0.13, and 0.07 for segment size ratios of 2, 4, and 8. It is difficult to decide a priori which segment size ratio is optimal for rheological properties, as decreasing the size of linear catalyst segments lowers the zero-shear viscosity but it also reduces strain hardening, and more experiments are needed, especially in extension, to decide the maximum size ratio. Nevertheless, plotting the ratio of the relative weight of inner backbones $\check{\Phi}_B \times \check{M}_{WB}$ to that of free arms $\check{\Phi}_A \times \check{M}_{WA}$, as in Figure 12, gives a rough qualitativeidea of the impact on strain hardening and rheology. We note that for segment size ratios of 4 and 8, this "rheological weight" of inner backbones decreases at low values of ps_2, while it is significantly lower and roughly constant for the segment size ratio 2. In Figure 12, the continuous curve (respectively the dashed curve) is the locus where the weight fraction of inner backbones (respectively free arms) is the same as at point β_2^* in Figure 11. The arrows indicate the domain where properties are improved, i.e., where the weight fraction of inner backbones is increased, and the fraction of free arms reduced. In terms of composition ps_2, the width of this domain decreases for $M^*_{N,S2}/M^*_{N,S1}$ larger than 4, allowing less freedom in the choice of parameters. Thus, we assume that $M^*_{N,S2}/M^*_{N,S1} = 4$ may be an interesting compromise, especially around

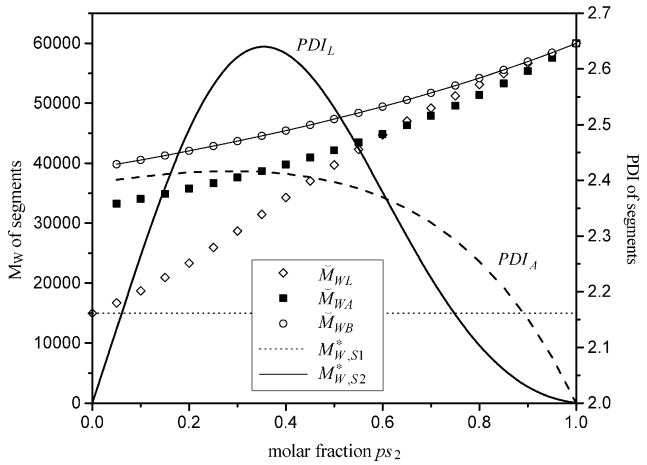

Figure 13. Variation of weight-average molecular weights and polydispersity indices of segments vs molar fraction of catalyst 2 for $v_1/v_2 = 3.4$ along curve $M^*_{N,S2}/M^*_{N,S1} = 4$ of Figure 11.

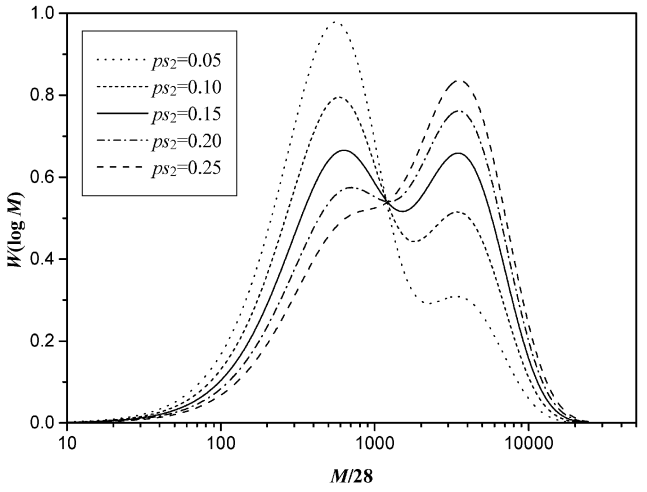

Figure 14. Evolution of MWD with molar fraction ps_2 for $v_1/v_2 = 3.4$ and $M^*_{N,S2}/M^*_{N,S1} = 4$ (see Figure 12). All distributions were checked by Monte Carlo simulation.

$ps_2 = 0.15$, i.e., just inside the domain marked by the arrows in Figure 12.

The evolution of the weight-average MW of linear chains, free arms, and inner backbones must also be taken into account and are plotted in Figure 13, together with weight-average MW of segments from catalysts 1 and 2. The segment size for the linear catalyst is independent of ps_2, but the segment size for the LCB catalyst increases with ps_2, reflecting the fact that for low values of ps_2 the amount of macromonomer is much larger than at large ps_2, leading to more frequent branching as indicated by eqs 86 and 87. The size of inner backbones is identical to that of LCB−CGC segments and they have a polydispersity index of 2, whereas linear chains and free arms are intermediate between $M^*_{W,S1}$ and $M^*_{W,S2}$, and their polydispersity indices are shown in Figure 13. Below $ps_2 = 0.3$, the size ratio of inner backbones to free arms is roughly constant so that the main effect seen in Figure 12 results from segmental composition.

The final information needed to establish the best composition for a given application is the MWD. Figure 14 shows predictions of the model (see Appendix B) for several mole fractions of LCB catalyst for a segment size ratio of 4. The distributions are bimodal, with

Table 3. Comparison of Parameters for HDB4 INSITE Sample and a Combined System of Two Catalysts[a]

	HDB4	combined system
$\check{M}_{WL}$:PDI$_L$	54 100:2.00	27419.4:2.39
$\check{M}_{WA}$:PDI$_A$	54 100:2.00	45710.5:2.41
$\check{M}_{WB}$:PDI$_B$	54 100:2.00	54090.7:2.00
M_W:PDI	96 000:2.45[b]	80962.6:4.42
LCB/1000C	0.080	0.115
$\bar{\beta}$	0.224	0.149
$\check{\Phi}_L$	0.5837	0.5783
$\check{\Phi}_A$	0.3684	0.3138
$\check{\Phi}_B$	0.0479	0.1079

[a] $\beta^*_1 = 0$, $\beta^*_2 = 0.4$, $v_1/v_2 = 3.4$, $M^*_{N,S2}/M^*_{N,S1} = 4$, $M^*_{N,S2} = 39\,200$, $ps_2 = 0.15$. [b] The PDI obtained from GPC is 2.14. We instead use the value obtained from M_W and LCB/1000C, which are considered more reliable (see ref 1).

PDI reaching a maximum of 4.42 at $ps_2 = 0.15$. It was found that bimodality disappears only for segment size ratios below 2.5 and that replacing the linear catalyst by a low-β LCB catalyst does not affect the bimodality significantly. Nevertheless, bimodality combined with long-chain branching should allow good control of processability. If a monomodal MWD is required, a third catalyst with intermediate β could be used.

Finally we compare the main expected characteristics for the 2 catalyst-system described above with an actual sample referred to as HDB4 in ref 1. This sample is one of a series of INSITE single-site catalyst resins made by Dow Chemical having increasing branching densities. These materials have been thoroughly characterized, and their properties have been published elsewhere.[25−27] This resin was chosen because it exhibits significant strain hardening, whereas no or very little hardening is observed for other resins in the series that have lower branching levels. From the values of M_W from LALLS and LCB/1000C from NMR, one can determine the values of β and $M_{N,S}$ from which all the parameters listed in Table 3 can be calculated. The weight $M^*_{N,S2}$ was increased to 39 300 so that inner backbones in the combined system would have the same MW as HDB4. We obtain an overall weight-average MW lower than HDB4 with a higher PDI. Free arms are shorter in the combined system, with a slightly lower fraction, whereas the weight fraction of inner backbones is more than twice that of HDB4. The "rheological weight" of inner backbones, $(\check{\Phi}_B\check{M}_{WB})/(\check{\Phi}_A\check{M}_{WA})$, equals 0.407 for the combined system, vs 0.130 for HDB4, which indicates that strain hardening will probably be increased compared to HDB4, while keeping the zero-shear viscosity reasonably low. Larger values of β^*_2 would certainly give similar, or even better results. Once again, this is only a coarse prediction, since experimental rheological results on combined systems have not yet been published. A last remark concerns the value of $\bar{\beta}$ from eq 28, which is lower for the combined system, although the branching density is higher, due to a lower number-average molecular weight. This means that for the same number of molecules, fewer branch points are created for the combined system, due to the larger number of linear molecules. However, these branch points create more inner backbones than a single LCB catalyst, because the number of molecules with few branch points is reduced significantly, and in their place, more highly branched, comblike molecules are formed.

Conclusion

We present a model describing completely the statistics of materials produced by combined systems of any number of single-site catalysts producing either linear or branched polymer. It consists of an analytical solution of a Monte Carlo simulation and is intended to provide the topological information necessary to estimate qualitatively the melt rheological behavior in shear and extensional flow, by emphasizing the role of linear chains, free arms, and inner backbones. The overall molecular weight distribution obtained by Monte Carlo simulations can be closely approximated using a new method which allow much faster computations.

An example of optimization of parameters for a two-catalyst system is presented in the simple case of a linear catalyst−LCB catalyst combination. The choice of optimal parameters must still be guided by experimental data, but it is shown that the linear catalyst must form chains that are shorter than segments of the LCB catalyst and with a larger fraction of vinyl-ended molecules. It seems likely that optimal two-catalyst systems will yield bimodal distributions.

To make the multiple-catalyst optimization procedure rigorous, a better understanding of the influence of free arms and inner backbones on strain hardening is required. Future work will make use of the statistical results on segment composition and size distribution predicted by the model for single and multiple catalyst to obtained more quantitative rheological prediction using various tube models.[5,6,8] The model could be developed further to predict the amount of comb molecules formed or the seniority distribution, or to include different reactivities for macromonomers according to their size.

Acknowledgment. The author is grateful to Professor John Dealy (McGill University) and to Professor Paula Wood-Adams (Concordia University) for many useful discussions, and thanks the Dow Chemical Company for permission to publish this work.

Appendix A: Weight Average Molecular Weights

The weight-average molecular weight, $\check{M}_W(n)$, of molecules with nBP is derived by a method somewhat similar to that for $\check{M}_N(n)$, which uses the general principal of blending for the number-average molecular weights. If we blend k resins with number and weight-average molecular weights M_{Ni} and M_{Wi}, each with a molar fraction F_{Ni} (and weight fraction F_{Wi}), the average number and weight MW for the blend are given by

$$M_N = \sum_{i=1}^{k} F_{Ni} M_{Ni} \tag{A1}$$

$$M_W = \sum_{i=1}^{k} F_{Wi} M_{Wi} \tag{A2}$$

with

$$F_{Wi} = \frac{F_{Ni} M_{Ni}}{\sum_{i=1}^{k} F_{Ni} M_{Ni}} = F_{Ni} \frac{M_{Ni}}{M_N} \tag{A3}$$

Equation 73 made implicit use of eq A1 and of the fact that mole fractions act as probabilities, so that they can be multiplied to obtain the probability of the newly formed molecule. As weight fractions do not have this property, we combine eq A2 and A3 to obtain a blending rule using mole fractions:

$$M_N M_W = \sum_{i=1}^{k} F_{Ni} M_{Ni} M_{Wi} \tag{A4}$$

Instead of using the weight $\check{W}^{(i)}(n)$ as in eq 71−73, we introduce $\check{Z}^{(i)}(n)$, defined as

$$\check{Z}^{(i)}(n) = \mathrm{Pb}_i \sum_{k=0}^{n-1} \check{F}_N^{=}(k) \check{F}_N^{(i)}(n-k-1) \times \check{M}_{NW}^{(i)}(0,k,n-k-1) \tag{A5}$$

where $\check{M}_{NW}^{(i)}(0, k, n-k-1)$ is the product of the number and weight-average molecular weights of the molecule formed by the conjunction of a linear segment from site i, a vinyl-terminated molecule with k branch points, and a molecule from site i with $n-k-1$ branch points.

We are left with the problem of finding the weight-average molecular weight of a three-arm star, each arm j having a different MWD, for which we know only M_{Nj} and M_{Wj}.

Assuming that the number distribution for the size of an arm j is $P_j(M_j)$, the following definitions apply for the mean, variance and variance about zero:

$$\mu_{1j} = \int_0^\infty M_j P_j(M_j)\, \mathrm{d}M_j = M_{Nj} \tag{A6}$$

$$\sigma_j^2 = \int_0^\infty (M_j - M_{Nj})^2 P_j(M_j)\, \mathrm{d}M_j \tag{A7}$$

$$\mu_{2j} = \int_0^\infty M_j^2 P_j(M_j)\, \mathrm{d}M_j = M_{Nj} M_{Wj} \tag{A8}$$

The classical relation between the variances about the mean and about zero applies, and

$$\mu_{2j} = \sigma_j^2 + \mu_{1j}^2 \tag{A9}$$

As the number distribution for the three-arm star is the distribution of the sum of three random variables, the overall mean and variance satisfy:

$$\mu_1 = \sum_{j=1}^{3} \mu_{1j} \quad \text{and} \quad \sigma^2 = \sum_{j=1}^{3} \sigma_j^2 \tag{A10}$$

Then introducing M_N and M_W for the three-arm star, we obtain

$$M_N = \mu_1 = \sum_{j=1}^{3} M_{Nj} \tag{A11}$$

$$M_N M_W = \mu_2 = \sigma^2 + \mu_1^2 = \sum_{j=1}^{3} (M_{Nj} M_{Wj} - M_{Nj}^2) + \left(\sum_{j=1}^{3} M_{Nj}\right)^2 \tag{A12}$$

Returning to the original problem, we find the recurrence relation

$$\check{Z}^{(i)}(n) = \mathrm{Pb}_i \sum_{k=0}^{n-1} \check{F}_{\mathrm{N}}^{=}(k)\check{F}_{\mathrm{N}}^{(i)}(n-k-1) \times \check{M}_{\mathrm{NW}}^{(i)}(0,k,n-k-1) \quad \text{(A13)}$$

$$\check{M}_{\mathrm{NW}}^{(i)}(0,k,n-k-1) = \check{M}_{\mathrm{N}}^{(i)}(0)\check{M}_{\mathrm{W}}^{(i)}(0) + \check{M}_{\mathrm{N}}^{=}(k)\check{M}_{\mathrm{W}}^{=}(k) + \check{M}_{\mathrm{N}}^{(i)}(n-k-1)\check{M}_{\mathrm{W}}^{(i)}(n-k-1) + 2\check{M}_{\mathrm{N}}^{(i)}(0)\check{M}_{\mathrm{N}}^{=}(k) + 2\check{M}_{\mathrm{N}}^{=}(k)\check{M}_{\mathrm{N}}^{(i)}(n-k-1) + 2\check{M}_{\mathrm{N}}^{(i)}(n-k-1)\check{M}_{\mathrm{N}}^{(i)}(0) \quad \text{(A14)}$$

$$\check{Z}(n) = \sum_{i=1}^{q} \mathrm{ps}_i b_i \check{Z}^{(i)}(n) \quad \text{(A15)}$$

$$\check{Z}^{=}(n) = \sum_{i=1}^{q} \mathrm{ps}_i a_i \check{Z}^{(i)}(n) \quad \text{(A16)}$$

$$\check{M}_{\mathrm{W}}^{=}(j) = \frac{\check{Z}^{=}(j)}{\check{W}^{=}(j)} \quad \text{(A17)}$$

$$\check{M}_{\mathrm{W}}^{(i)}(j) = \frac{\check{Z}^{(i)}(j)}{\check{W}^{(i)}(j)} \quad \text{(A18)}$$

with the following initialization

$$\check{M}_{\mathrm{W}}^{(i)}(0) = M_{\mathrm{W,S}i} = 2M_{\mathrm{N,S}i} \quad \text{(A19)}$$

$$\check{Z}^{(i)}(0) = \check{F}_{\mathrm{N}}^{(i)}(0)\check{M}_{\mathrm{N}}^{(i)}(0)\check{M}_{\mathrm{W}}^{(i)}(0) = 2\check{F}_{\mathrm{N}}^{(i)}(0)M_{\mathrm{N,S}i} \quad \text{(A20)}$$

Finally, the weight-average molecular weight for molecules with n branch points is obtained by

$$\check{M}_{\mathrm{W}}(n) = \frac{\check{Z}(n)}{\check{W}(n)} \quad \text{(A21)}$$

and the overall weight-average molecular weight follows:

$$M_{\mathrm{w}} = \sum_{n=1}^{\infty} \check{F}_{\mathrm{W}}(n)\check{M}_{\mathrm{W}}(n) \quad \text{(A22)}$$

Despite the apparent complexity of this recurrence, the values of $\check{M}_{\mathrm{N}}(n)$, $\check{M}_{\mathrm{W}}(n)$, $\check{F}_{\mathrm{N}}(n)$, and $\check{F}_{\mathrm{W}}(n)$ can be obtained by a subroutine containing fewer than 100 lines of code (an Excel Visual Basic macro can be obtained from the author upon request).

Appendix B: Approximate Molecular Weight Distribution

Computing the MWD of the whole system requires knowledge of all the number distributions $P_{\mathrm{N}}(M,n)$ of molecules with n branch points and molecular weights M. It is straightforward for $n = 0$, reasonably easy for $n = 1$, but very tedious if not impossible for $n \geq 2$. Nevertheless, we note that the polydispersity index $\check{M}_{\mathrm{W}}(n)/\check{M}_{\mathrm{N}}(n)$ decreases quite quickly with n. In Figure 15, we compare this result for a combination of two

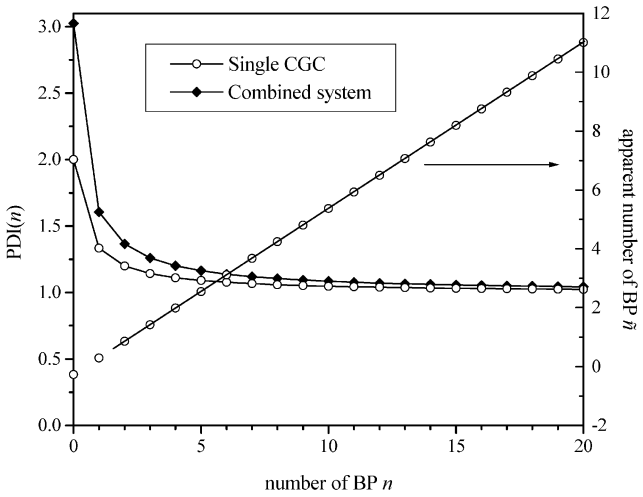

Figure 15. Variation of polydispersity index and apparent index $\tilde{n}$ (from eq B3) with number of branch points: comparison between the case of a single CGC and multiple CGC ($\beta_1 = 0.43$, $\beta_2 = 0$, $M_{\mathrm{N,S2}}/M_{\mathrm{N,S1}} = 1.9$, $\nu_2/\nu_1 = 0.5$, $\mathrm{ps}_2 = 0.15$).

LCB−CGC with the case of a single site catalyst, for which we have[1]

$$\frac{M_{\mathrm{W}}(n)}{M_{\mathrm{N}}(n)} = \frac{2n+2}{2n+1} \quad \text{(B1)}$$

In the two-catalyst system, as the segment average sizes differ, the polydispersity of molecules with n branch points is larger than for the single catalyst, but the shape is similar; when the number of branch points increases, the molecules become more and more monodisperse. It is then attempting to find for the multiple catalyst system the apparent value of n, denoted $\tilde{n}$, that would lead to the same polydispersity for a single site catalyst:

$$\frac{\check{M}_{\mathrm{W}}(n)}{\check{M}_{\mathrm{N}}(n)} = \frac{2\tilde{n}+2}{2\tilde{n}+1} \quad \text{(B2)}$$

or equivalently

$$\tilde{n} = \frac{\check{M}_{\mathrm{N}}(n) - \check{M}_{\mathrm{W}}(n)/2}{\check{M}_{\mathrm{W}}(n) - \check{M}_{\mathrm{N}}(n)} \quad \text{(B3)}$$

$\tilde{n}$ is smaller than n, and the relation between the two variables is represented in Figure 15. We find fairly linear behavior, especially for $n \geq 2$.

In the case of a single catalyst, it was found that the number distribution of molecules with n branch points, or number bivariate distribution, follows the classical Γ distribution

$$P_{\mathrm{N}}(M,n) = P_{\Gamma}(M,2n+1,M_{\mathrm{N,S}}) \quad \text{(B4)}$$

where

$$P_{\Gamma}(x,\alpha,x_0) = \frac{x^{\alpha-1}}{\Gamma(\alpha){x_0}^{\alpha}} \exp(-x/x_0) \quad \text{(B5)}$$

and $\Gamma(\alpha) = (\alpha - 1)!$ when α is an integer.

Then for molecules with n branch points, we can construct an approximate number bivariate distribution

that has the correct number and weight-average molecular weights by setting

$$Q_N(M,n) = P_\Gamma(M,2\tilde{n}+1,\tilde{M}_{N,S}) \quad \text{(B6)}$$

with

$$\tilde{M}_{N,S} = \frac{\check{M}_N(n)}{2\tilde{n}+1} \quad \text{(B7)}$$

The overall number distribution is then

$$N(M) = \sum_{n=0}^{\infty} \check{F}_N(n) Q_N(M,n) \quad \text{(B8)}$$

and the molecular weight distribution reads:

$$W(M) = \frac{M}{M_N} N(M) \quad \text{(B9)}$$

Using the approximation of eq B6 we expect to introduce only a small error for large values of n, but a very significant error for linear chains. Indeed, for two catalysts in particular, if $M_{N,S1}$ and $M_{N,S2}$ are quite different, the distribution of linear chains will be bimodal, which cannot be captured by the Γ function. Bimodality could also occur for stars if, for instance, one site produces very long linear chains (linear-CGC), and the other produces branched molecules with short segments (LCB−CGC); the two kinds of star that would be made by the LCB−CGC, with branches coming from either the linear-CGC or the LCB−CGC, could have sufficiently different average molecular weights so that their distribution would be bimodal, or at least strongly distorted. For molecules with more branch points, all possible reaction routes tend to smooth the distributions so that no bimodality is observed.

To deal with the bimodality, we can compute the exact distribution for linear molecules and for stars.

The number fraction of linear chains from site i is simply given by

$$f_N^{(i)}(0) = \frac{ps_i b_i \check{F}_N^{(i)}(0)}{\check{F}_N(0)} \quad \text{(B10)}$$

and their number distribution is

$$P_N^{(i)}(M,0) = \frac{\exp(-M/M_{N,Si})}{M_{N,Si}} \quad \text{(B11)}$$

The number distribution for all linear chains is, therefore:

$$Q_N(M,0) = \sum_{i=1}^{q} f_N{}^{(i)}(0) P_N^{(i)}(M,0) \quad \text{(B12)}$$

We proceed similarly for stars. Stars made by site i will have a number fraction

$$f_N{}^{(i)}(1) = \frac{ps_i b_i \check{F}_N^{(i)}(1)}{\check{F}_N(1)} = \frac{ps_i b_i Pb_i(1-Pb_i)\check{F}_N^{=}(0)}{\check{F}_N(1)} \quad \text{(B13)}$$

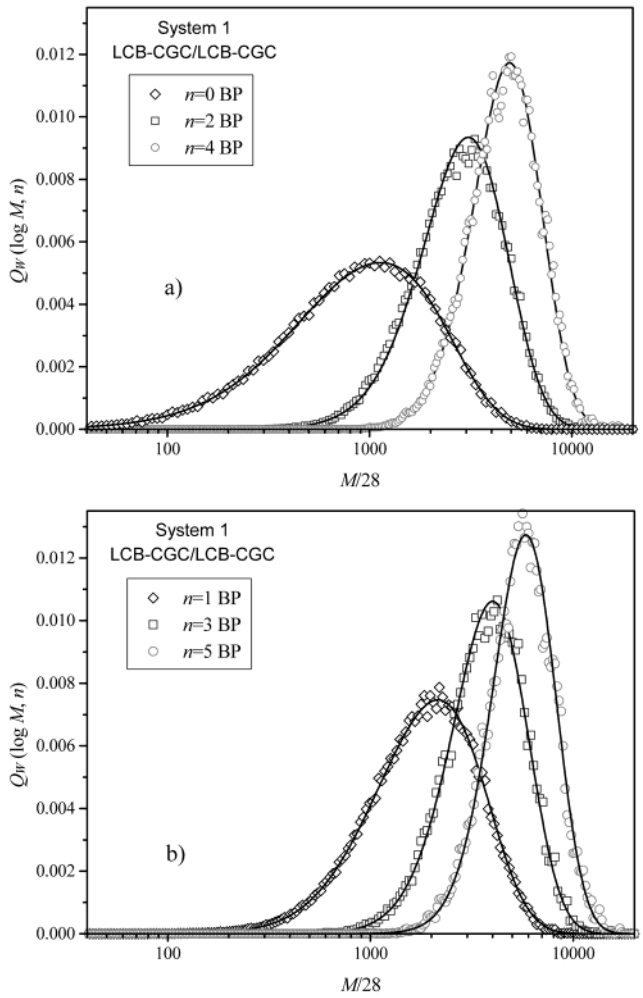

Figure 16. Verification of model (lines) for molecular weight distribution of molecules with 0 to 5 branch points by comparison with Monte Carlo simulation (symbols) for system 1 ($\beta_1 = 0.43$, $\beta_2 = 1$, $M_{N,S1}/28 = 256.6$, $M_{N,S2}/28 = 666.7$, $\nu_1 = 1$, $\nu_2 = 0.5$, $ps_1 = 0.5$).

The term $\check{F}_N^{=}(0)$ takes into account the probability of having a branch from any site j, and is found by

$$\check{F}_N^{=}(0) = \sum_{j=1}^{q} ps_j a_j (1 - Pb_j) \quad \text{(B14)}$$

We then obtain the number fraction of stars made by site i and containing a branch from site j:

$$f_N^{(i,j)}(1) = \frac{ps_i b_i Pb_i(1-Pb_i) ps_j a_j (1-Pb_j)}{\check{F}_N(1)} \quad \text{(B15)}$$

The number distribution of such molecules is obtained by

$$P_N^{(i,j)}(M,1) = \int_0^M dx\, P_N^{(i)}(x)\left[\int_0^{M-x} dy\, P_N^{(j)}(y) P_N^{(j)}(M-x-y)\right] \quad \text{(B16)}$$

assuming that the two segments from site i have weights x and y, and the branch from site j is of weight $M-x-y$. We note that the relation above is a convolution:

$$P_N^{(i,j)}(M,1) = P_N^{(i)}(M,0) * P_N^{(i)}(M,0) * P_N^{(j)}(M,0) \quad \text{(B17)}$$

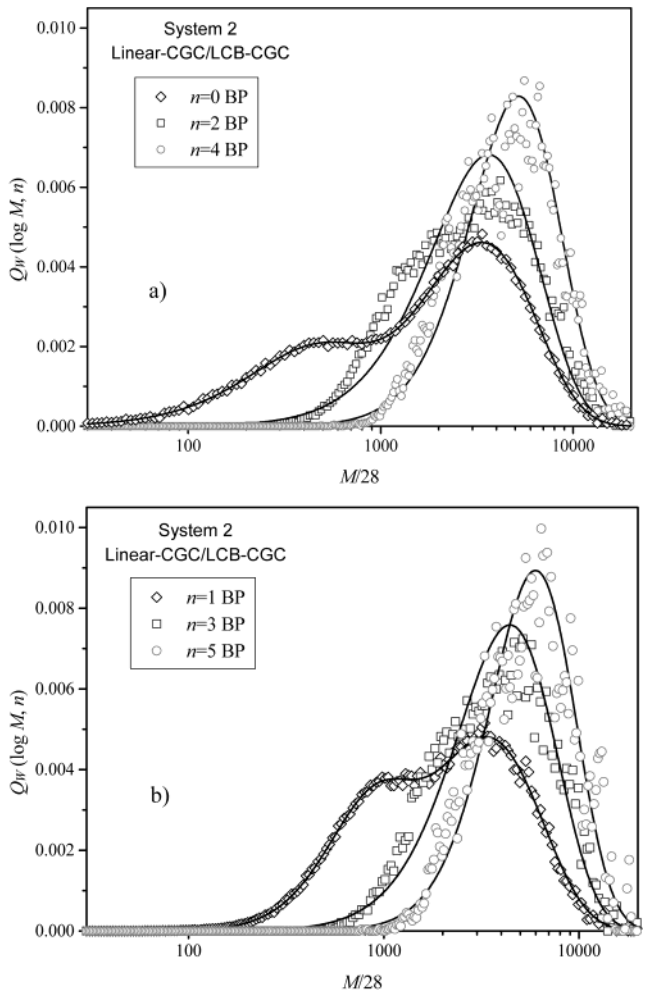

Figure 17. Verification of model (lines) for molecular weight distribution of molecules with 0 to 5 branch points by comparison with Monte Carlo simulation (symbols) for system 2 ($\beta_1 = 0.332$, $\beta_2 = 0$, $M_{N,S1}/28 = 200.1$, $M_{N,S2}/28 = 1666.7$, $\nu_1 = 0.5$, $\nu_2 = 1$, $ps_1 = 0.75$).

where * is the convolution operator. Instead of integrating, we use the property of the Laplace transform

$$\mathcal{L}[P_N^{(i,j)}(M,1)](s) = \mathcal{L}[P_N^{(i)}(M,0)](s)\mathcal{L}[P_N^{(i)}(M,0)](s)\mathcal{L}[P_N^{(j)}(M,0)](s) = [(1 + sM_{N,Si})(1 + sM_{N,Si})(1 + sM_{N,Sj})]^{-1} \quad \text{(B18)}$$

Expanding and inverting the Laplace transform gives

$$P_N^{(i,j)}(M,1) = \begin{cases} \dfrac{M^2}{2(M_{N,Si})^3}E_i & \text{if } j = i \\ \dfrac{M_{N,Sj}(E_j - E_i)}{(M_{N,Sj} - M_{N,Si})^2} - \dfrac{ME_i}{M_{N,Si}(M_{N,Sj} - M_{N,Si})} & \text{if } j \neq i \end{cases} \quad \text{(B19)}$$

where E_i is a shortened notation for $\exp(-M/M_{N,Si})$.

Then for all three-arm stars the number bivariate distribution reads:

$$Q_N(M,1) = \sum_{\substack{i=1 \\ j=1}}^{q} f_N^{(i,j)}(M,1)P_N^{(i,j)}(M,1) \quad \text{(B20)}$$

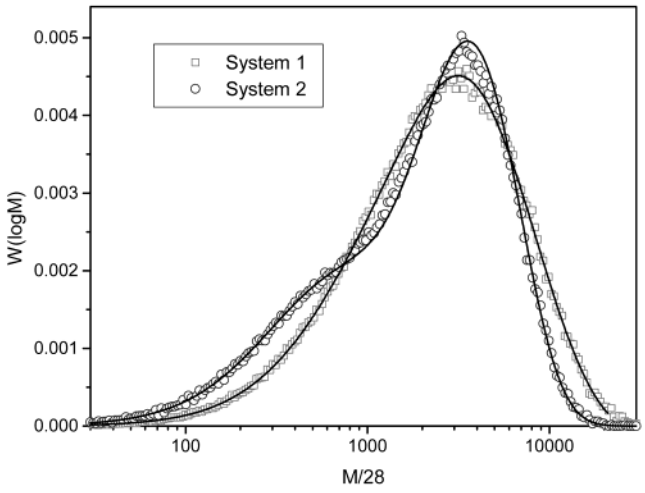

Figure 18. Overall MWD for systems 1 and 2. Symbols correspond to Monte Carlo simulation and lines to the model. The polydispersity indices for systems 1 and 2 are 3.2 and 3.9, respectively.

For $n \geq 2$, we use the approximation $Q_N(M,n)$ from eq B6. The weight bivariate distribution $Q_W(M,n)$ is obtained by multiplying $Q_N(M,n)$ by $M/\check{M}_N(n)$.

Figures 16 and 17 show the results for two systems, the parameters of which are listed Table 2. System 1 is a combination of two CGC producing branched molecules to different extents, with a ratio of segment weights of about 2.5 in favor of the catalyst producing more branch points. It can be seen in Figure 16 that for $n = 0$ and $n = 1$, corresponding to linear chains and three-arm stars, we have very good agreement between the Monte Carlo results and values calculated by eq B12 and B20. For other values of n, although this time we use the approximation of eq B6, the agreement remains very satisfactory. To test the approximation in conditions where we expect that bimodality could affect the precision, we chose in system 2 a combination of a LCB−CGC giving significant branching and small segments, and a linear catalyst producing much longer chains (about 8 times longer than the segments of the LCB−CGC). We set the molar fraction of LCB−CGC equal to 0.75 to give a bimodal MWD of linear chains. In Figure 17, the exact model for $n = 0$ and $n = 1$ coincides exactly with the Monte Carlo results. On the contrary, for $n = 2$, $n = 3$ and $n = 4$, Monte Carlo results give a distorted MWD that the approximate model cannot reproduce. It gets better for $n = 5$.

The overall molecular weight distributions predicted by Monte Carlo simulations and by the present model are shown for these two systems in Figure 18. The good agreement for system 1 is not surprising considering the results of Figure 16. More interesting is the accurate prediction that the approximate model provides for system 2, despite the fact the bivariate distributions for intermediate values of n were unsatisfactory. This shows that the approximate solution for the MWD might be quite accurate for systems of catalysts where bimodality is not purposely sought.

Nomenclature of Main Symbols

β_i	average number of BP per molecule for catalyst i in the mixture

β_i^* average number of BP per molecule for catalyst i when used alone ($ps_i = 1$)

$\bar{\beta}$ average number of BP per molecule in the combined system

λ_i^* branching density that catalyst i would achieve if used alone ($ps_i = 1$)

λ branching density [LCB/1000C] in the combined system

$\phi_{L,i}$, $\phi_{A,i}$, $\phi_{B,i}$ number or weight fraction of linear segments, free arms, and inner backbones for a single catalyst i

Φ_A, $\check{\Phi}_A$ weight fraction of free arms in the case of complete and partial vinyl termination

Φ_B, $\check{\Phi}_B$ weight fraction of inner backbones in the case of complete and partial vinyl termination

Φ_L, $\check{\Phi}_L$ weight fraction of linear segments in the case of complete and partial vinyl termination

a_i effective vinyl termination probability (eq 65)

b_i reactivity probability (eq 64)

$b(m)$ number fraction of main backbones with m branch points

$b_i(m)$ number fraction of main backbones from catalyst i with m branch points

$F_N(n)$, $\check{F}_N(n)$ number fraction of molecules with n branch points in the case of complete and partial vinyl termination

$\check{F}_N^=(n)$ number fraction of vinyl-ended molecules with n BP made by catalyst i in the case of partial vinyl termination

$F_N^{(i)}(n)$, $\check{F}_N^{(i)}(n)$ number fraction of molecules with n BP made by catalyst i in the case of complete and partial vinyl termination

$\check{F}_W(n)$ weight fraction of molecules with n BP in the case of partial vinyl termination

lp_i monomer selection probability for catalyst i

lp_i^* monomer selection probability for catalyst i when used alone ($ps_i = 1$)

m number of BP in a given main backbone

M_N, M_W overall number and weight MW of the combined system

$M_{N,Si}$ number-average MW of segments between BP for catalyst i in the mixture

$M_{N,Si}^*$ number-average MW of segments between BP for catalyst i used alone ($ps_i = 1$)

$\check{M}_N^{(i)}(n)$ number-average MW of molecules with nBP made by catalyst i

$\check{M}_N^=(n)$ number-average MW of vinyl-ended molecules with nBP

$\check{M}_N(n)$, $\check{M}_W(n)$ number- and weight-average MW in the case of partial vinyl termination

$\check{M}_{NA}$, $\check{M}_{WA}$ number and weight-average MW of free arms for partial vinyl termination

$\check{M}_{NB}$, $\check{M}_{WB}$ number- and weight-average MW of inner backbones for partial vinyl termination

$\check{M}_{NL}$, $\check{M}_{WL}$ number- and weight-average MW of linear segments for partial vinyl termination

n number of branch points in a given molecule

$n^=$ number of vinyl-ended main backbones

n_a number of main backbones containing branch points

$n_a^=$ number of vinyl-terminated main backbones containing branch points

n_b number of inner backbones in main backbones

n_l number of linear chains among main backbones

$n_l^=$ number of vinyl terminated linear chains among main backbones

N number of main backbones before grafting

N_L, $\check{N}_L$ number of linear segments for complete and partial vinyl termination

N_A, $\check{N}_A$ number of free arms for complete and partial vinyl termination

N_B, $\check{N}_B$ number of inner backbones for complete and partial vinyl termination

N_{BP} number of branch points in the combined system

N_S total number of segments in the combined system

N_C total number of molecules in the combined system

pp_i propagation probability for catalyst i

pp_i^* propagation probability for catalyst i when used alone ($ps_i = 1$)

Pb_i Flory's branching probability for catalyst i in the reactor

ps_i mole fraction of catalyst i

R random number between 0 and 1

q number of catalysts in combined system

v_i vinyl termination probability for catalyst i

w_a weight of main backbones containing branch points

$w_a^=$ weight of vinyl-ended main backbones containing branch points

w_b weight of inner segments in main backbones

w_l weight of linear chains among main backbones

$w_l^=$ weight of vinyl-ended linear chains among main backbones

W_L, $\check{W}_L$ weight of linear segments for complete and partial vinyl termination

W_A, $\check{W}_A$ weight of free arms for complete and partial vinyl termination

W_B, $\check{W}_B$ weight of inner backbones for complete and partial vinyl termination

W_S total weight of segments in the combined system

References and Notes

(1) Costeux, S.; Wood-Adams, P. *Macromolecules* **2002**, *35*, 2514.
(2) Pattamaprom, C.; Larson, R. G. *Rheol. Acta* **2001**, *40*, 516.
(3) Léonardi, F.; Majesté, J.-C.; Allal, A.; Marin, G. *J. Rheol.* **2000**, *44*, 675.
(4) Milner, S. T.; McLeish, T. C. B.; Young, R. N.; Hakiki, A.; Johnson, J. M. *Macromolecules* **1998**, *31*, 9345.
(5) Daniels, D. R.; McLeish, T. C. B.; Crosby, B. J.; Young, R. N.; Fernyhough, C. M. *Macromolecules* **2001**, *34*, 7025.
(6) Larson, R. G. *Macromolecules* **2001**, *34*, 4556−4571.
(7) Read, D. J.; McLeish, T. C. B. *Macromolecules* **2001**, *34*, 1928.
(8) McLeish, T. C. B.; Larson, R. G. *J. Rheol.* **1998**, *42*, 81.
(9) Lohse, D. J.; Milner, S. T.; Fetters, L. J.; Xenidou, M.; Hadjichristidis, N.; Mendelson, R. A.; García-Franco, C. A.; Lyon, M. K. *Macromolecules* **2002**, *35*, 3066.
(10) Au-Yeung, V. S.; Macosko, C. W.; Raju, V. R. *J. Rheol.* **1981**, *25*, 445.
(11) Lai, S. Y.; Wilson, J. R.; Knight, J. R.; Stevens, G. W.; Chum, P. W. S. U.S. Patent 5,272,236, 1993.
(12) Lai, S. Y.; Wilson, J. R.; Knight, J. R.; Stevens, G. W. U.S. Patent 5,665,800, 1997.
(13) Zhu, S.; Li, D. *Macromol. Theory Simul.* **1997**, *6*, 793.
(14) Beigzadeh, D. Long-chain branching in ethylene polymerization using combined metallocene catalyst systems, Ph.D. Thesis, Waterloo University, Canada, 2000.
(15) Beigzadeh, D.; Soares, J. B. P.; Hamielec, A. E. *J. Appl. Polym. Sci.* **1999**, *71*, 1753.
(16) Beigzadeh, D.; Soares, J. B. P.; Duever, T. A. *Macromol. Rapid Commun.* **1999**, *20*, 541.
(17) Soares, J. B. P. *Macromol. Theory Simul.* **2002**, *11*, 184.
(18) Simon, L. C.; Soares, J. B. P. *Macromol. Theory Simul.* **2002**, *11*, 222.
(19) Zhu and Li computed this fraction as 20% of all molecules with 3 branch points.

(20) Shiau, L. D. *Polymer* **2002**, *43*, 2835.
(21) Beigzadeh, D.; Soares, J. B. P.; Duever, T. A. *Macromol. Symp.* **2001**, *173*, 179.
(22) The graph of ref 18 corresponding to eq 88 shows slightly lower branching densities than Figure 9, although all parameters as supposedly the same.
(23) Raju, V. R.; Smith, G. G.; Marin, G.; Knox, J. R.; Graessley, W. W. *J. Polym. Sci., Phys. Ed.* **1979**, *17*, 1183.
(24) Carella, J. M.; Gotro, J. T.; Graessley, W. W. *Macromolecules* **1986**, *19*, 659.
(25) Wood-Adams, P. M.; Dealy, J. M.; deGroot, A. W.; Redwine, O. D. *Macromolecules* **2000**, *33*, 7489.
(26) Wood-Adams, P. M. *J. Rheol.* **2001**, *45*, 203.
(27) Wood-Adams, P. M.; Costeux, S. *Macromolecules* **2001**, *34*, 6281.

MA0208640